2013

Role of Nuclear Factor E2 Related Factor 2 (NRF2) in Development of Steatosis and Drug Transporter Alterations

Vijay RS More
University of Rhode Island, vrsmore@gmail.com

ROLE OF NUCLEAR FACTOR E2 RELATED FACTOR 2 (NRF2) IN DEVELOPMENT OF STEATOSIS AND DRUG TRANSPORTER ALTERATIONS

BY

VIJAY RS MORE

A DISSERTATION SUBMITTED IN PARTIAL FULFILLMENT OF THE REQUIREMENTS FOR THE DEGREE OF

DOCTOR OF PHILOSOPHY

IN

PHARMACOLOGY AND TOXICOLOGY

UNIVERSITY OF RHODE ISLAND

2013

DOCTOR OF PHILOSOPHY IN PHARMACOLOGY AND TOXICOLOGY

OF

VIJAY RS MORE

APPROVED:

Thesis Committee:

Major Professor: ANGELA L SLITT

NASSER H ZAWIA

THOMAS MANFREDI

KEITH T KILLINGBECK

DEAN OF THE GRADUATE SCHOOL

UNIVERSITY OF RHODE ISLAND

2013

ABSTRACT

Steatosis is fat deposition in liver arising from conditions like obesity, diabetes, and/or alcohol consumption. It is a benign condition with normal liver function, and can often be reversed. Both alcoholic and non-alcoholic liver steatosis can further progress to irreversible steatohepatitis to cirrhosis and substantial loss of liver function. Nuclear factor E2 related factor 2 (Nrf2) is a transcription factor known to combat oxidative stress in the cell. The contribution of Nrf2 to other cellular functions, such as lipid homeostasis is emerging. The work herein assessed how enhanced Nrf2 activity impacts progression of hepatic steatosis with long-term high fat diet (HFD) feeding. C57BL/6 and Keap1-Knockdown (Keap1-KD) mice, which exhibit enhanced Nrf2 activity, were fed a HFD for 24 weeks. Keap1-KD mice had higher body weight, liver weight and higher hepatic fat deposition. Lipogenic gene expression was also higher in livers of Keap1-KD mice fed HFD. Next, the work herein studied effect of steatosis and cirrhosis on Nrf2 and drug transporter expression in human livers. Transporters aid in hepatobiliary excretion of many drugs and toxic chemicals, and can be determinants of drug-induced liver injury. Alcohol cirrhosis increased efflux transporter mRNA and protein expression in human livers as compared to normal non-steatotic livers. It was observed that transporter expression alterations with steatosis were much less severe as compared to cirrhosis. In order to demonstrate the effects of these drug transporter and metabolizing enzyme alterations on pharmacokinetics, we conducted oral Bisphenol A (BPA) disposition study in diet-induced obese

mice. The mice were administered deuterated BPA orally and blood levels were detected for BPA and BPA metabolites at times after BPA administration. Increased BPA clearance was observed in DIO mice, as compared to lean controls, attributed to increased phase II conjugation enzyme Ugt and biliary efflux transporter Abcc2 expression.

In conclusion, constitutive activity of Nrf2 increases susceptibility to mice to develop liver steatosis; and human livers with steatosis and alcohol cirrhosis have altered expression of drug transporters, which may result in xenobiotic disposition alterations.

ACKNOWLEDGEMENTS

I would like to acknowledge everyone who have supported me, guided me, helped me and inspired me to achieve my goals during this pleasant journey of graduate school.

First of all, I would like to thank my advisor Dr. Angela Slitt for her enormous support and inspiration along with an opportunity to work in her lab. She has helped me mature as a scientist and as a human being. Her expert guidance and enthusiasm about work has always motivated me to finish work in timely manner, and with utmost quality and ethics. The large portion of credit of my academic achievements during PhD goes to her.

I also want to thank my defense committee- Dr. Naseer Zawia, Dr. Becky Sartini, Dr. Ayman-El Kattan, and Dr. Matt Delmonico for their continued support, and prompt guidance during comprehensive exams as well as thesis defense. I want to thank Dr. El-Kattan for his valuable input for manuscript 4 writing. I also want to thank our collaborators from URI- Dr. Roberta King and Dr. Ruitang Deng as well as our collaborators from outside the URI- Dr. Nathan Cherrington (U. Arizona), Dr. Lauren Aleksunes (EOHSI Rutgers), and Dr. Daniel Doerge (US FDA) for their contribution to multiple projects. I also want to thank RI INBRE and GSC facilities for making available necessary technology for advanced research.

I would also like to acknowledge my lab members- Jialin, Maureen, Wei, Ajay, Praji, Deanna, Laura, Pragati as well as part members Supriya, Joan and Maneesha for their help with animal work, lab meeting discussions, comments on the posters, manuscripts, comprehensive exam, an many more things along the way. I also want to thank lab undergraduate students, including Jen, Olivia, Erica, and Jamie who worked with me for various projects helping me gain valuable mentoring and leadership skills.

Lastly, I would like to acknowledge my family- mom, dad, my sisters and brother in laws who have always believed in me, motivated me and taught me the way to pursue a dream. Finally, I want to thank my lovely wife Praji, who has been there for me through all the ups and downs and kept me focused. She has been most wonderful partner in this journey.

PREFACE

The following dissertation titled “Role of nuclear factor E2 related factor 2 (Nrf2) in development of steatosis and drug transporter alterations” is presented in manuscript format. There are four manuscripts in this dissertation. First manuscript is introductory and serves as a general background for manuscript two, three and four. Manuscript two is formatted in *Free Radical Biology and Medicine (FRBM)* journal style, third manuscript is in *Drug Metabolism Disposition (DMD)* style, and fourth is in *J Biochemical Molecular Toxicology (JBMT)* style. Manuscripts two and three are published in peer-reviewed journals as of March 2013.

TABLE OF CONTENTS

LIST OF TABLES

LIST OF FIGURES

MANUSCRIPT 1: None

MANUSCRIPT 2

MANUSCRIPT 3

MANUSCRIPT 4

MANUSCRIPT 1:

NUCLEAR FACTOR E2 RELATED FACTOR 2 (NRF2) IN NON-ALCOHOLIC AND ALCOHOLIC LIVER DISEASE

Vijay R More and Angela L Slitt

Biomedical and Pharmaceutical Sciences, University of Rhode Island, Kingston, RI

NRF2:

Nuclear factor E2 related factor 2, Nrf2, is a transcription factor very well known for combating oxidative stress by inducing a battery of antioxidant genes. Nrf2 protects against oxidative stress at baseline levels, as well as, upon challenge by reactive oxygen species (ROS). ROS are integral part of normal physiological mechanisms. However, loss of redox balance causes generation of excess ROS, which can lead to cytotoxicity (1). ROS play a vital role in pathogenesis of variety of diseases, such as cirrhosis, diabetes, hypertension, and cancer, along with neurological disorders including Parkinson's disease (2), and Schizophrenia (3). As reviewed by Naik and Dixit (2011), ROS can also lead to deregulated inflammation, arising from production of pro-inflammatory cytokines (4).

Kelch like associated protein 1 (Keap1) acts as an inhibitor of Nrf2 by preventing its entry into nucleus to interact with antioxidant response element (ARE) (Fig. 1) (5). Keap1 contains multiple cysteine residues in its structure, which are excellent sites for electrophillic attack. The hinge and latch model described that one molecule of Nrf2 is sequestered to two molecules of Keap1, with one having more affinity for Nrf2 than other. Upon induction, the loose interaction between Nrf2 and one of the Keap1 is broken, and stronger one remains intact. Because of this structural modification of protein complex, degradation of Nrf2 by proteosome 26S is inhibited. This results in

Nrf2 accumulation to the extent that passes sequestering capacity of Keap1, and excess Nrf2 moves to nucleus (6).

NON-ALCOHOLIC FATTY LIVER DISEASE (NAFLD):

Owing to increasing prevalence of obesity and diabetes, NAFLD is becoming the most common liver disease (7). Youssef and McCullough reviewed the connections between obesity and NAFLD (8). The prevalence of NAFLD is 10-fold more in obese patients than in general population. Non-alcoholic steatohepatitis (NASH) is severe form of NAFLD, which can progress to fibrosis and cirrhosis. Insulin resistance is considered as key pathogenic factor in progression of NASH (9). NASH, the most severe form of NAFLD, is known to develop by two “hits” (10). The first hit is steatosis, which is fat deposition in liver, followed by second hit involving oxidative stress. Even though progression of liver from steatosis to NASH is incompletely understood, it is clear that oxidative stress plays the major role in the process (11). So, it is likely that Nrf2 exerts its protective actions in the second hit of the NASH, but acting to bolster expression of genes that encode for cytoprotective enzymes, which can counter oxidative stress, such as glutathione cysteine ligase, superoxide dismutase, and glutathione peroxidase. However, very little is known about whether Nrf2 plays any role in steatosis, the first hit of NASH.

ALCOHOLIC FATTY LIVER DISEASE:

Alcoholic liver disease is a spectrum of conditions ranging from simple steatosis to alcoholic steatohepatitis to alcoholic cirrhosis. Similar to obesity driven steatosis, alcoholic steatosis is also a reversible condition, and can be suppressed by abstinence from alcohol (12). Continued consumption of larger quantities of alcohol causes increase in inflammatory cytokine levels, increased bile acid levels in liver, leading to alcoholic hepatitis. There is severe hepatocyte ballooning because of excessive amount of water (13). There is increase in oxidative stress in the liver, and this may lead to fibrosis of liver. Excessive scar tissue formation leads to cirrhotic liver, wherein significant loss of liver function occurs. Alcoholic cirrhosis is completely irreversible damage of the liver tissue, and eventually leads to liver failure (13). According to Center for Disease Control and prevention (CDC), more than 15,000 Americans die every year from alcoholic liver cirrhosis (National Vital Statistics Report, Volume 60, No 3).

About 30% of cirrhotic patients also suffer from diabetes (14). Acute, as well as chronic alcohol consumption leads to development of insulin resistance, which can progress to diabetes mellitus (15). Disruption of normal functions of the liver in cirrhosis may lead to hepatogenous diabetes (16). Additionally, obesity and diabetes mellitus increase the severity of alcoholic liver disease (17). Owing to interplay between diabetes and cirrhosis, the two conditions often co-present clinically (18).

REFERENCES:

1. Whaley-Connell A, McCullough PA, Sowers JR. The role of oxidative stress in the metabolic syndrome. Rev Cardiovasc Med 2011;12(1):21-9.
2. Schapira AH, Jenner P. Etiology and pathogenesis of Parkinson's disease. Mov Disord 2011;26(6):1049-55.
3. Mico JA, Rojas-Corrales MO, Gibert-Rahola J, Parellada M, Moreno D, Fraguas D, Graell M, Gil J, Irazusta J, Castro-Fornieles J and others. Reduced antioxidant defense in early onset first-episode psychosis: a case-control study. BMC Psychiatry 2011;11:26.
4. Naik E, Dixit VM. Mitochondrial reactive oxygen species drive proinflammatory cytokine production. J Exp Med 2011;208(3):417-20.
5. Itoh K, Wakabayashi N, Katoh Y, Ishii T, Igarashi K, Engel JD, Yamamoto M. Keap1 represses nuclear activation of antioxidant responsive elements by Nrf2 through binding to the amino-terminal Neh2 domain. Genes Dev 1999;13(1):76-86.
6. Tong KI, Kobayashi A, Katsuoka F, Yamamoto M. Two-site substrate recognition model for the Keap1-Nrf2 system: a hinge and latch mechanism. Biol Chem 2006;387(10-11):1311-20.
7. Della Corte C, Alisi A, Iorio R, Alterio A, Nobili V. Expert opinion on current therapies for nonalcoholic fatty liver disease. Expert Opin Pharmacother 2011.

8. Youssef WI, McCullough AJ. Steatohepatitis in obese individuals. Best Pract Res Clin Gastroenterol 2002;16(5):733-47.

9. Mehta K, Van Thiel DH, Shah N, Mobarhan S. Nonalcoholic fatty liver disease: pathogenesis and the role of antioxidants. Nutr Rev 2002;60(9):289-93.

10. Tessari P, Coracina A, Cosma A, Tiengo A. Hepatic lipid metabolism and non-alcoholic fatty liver disease. Nutr Metab Cardiovasc Dis 2009;19(4):291-302.

11. Koek GH, Liedorp PR, Bast A. The role of oxidative stress in non-alcoholic steatohepatitis. Clin Chim Acta 2011;412(15-16):1297-305.

12. Teli MR, Day CP, Burt AD, Bennett MK, James OF. Determinants of progression to cirrhosis or fibrosis in pure alcoholic fatty liver. Lancet 1995;346(8981):987-90.

13. Walsh K, Alexander G. Alcoholic liver disease. Postgrad Med J 2000;76(895):280-6.

14. Hickman IJ, Macdonald GA. Impact of diabetes on the severity of liver disease. Am J Med 2007;120(10):829-34.

15. Kim SJ, Kim DJ. Alcoholism and diabetes mellitus. Diabetes Metab J 2012;36(2):108-15.

16. Garcia-Compean D, Jaquez-Quintana JO, Gonzalez-Gonzalez JA, Maldonado-Garza H. Liver cirrhosis and diabetes: risk factors, pathophysiology, clinical implications and management. World J Gastroenterol 2009;15(3):280-8.

17. Raynard B, Balian A, Fallik D, Capron F, Bedossa P, Chaput JC, Naveau S. Risk factors of fibrosis in alcohol-induced liver disease. Hepatology 2002;35(3):635-8.

18. Baig NA, Herrine SK, Rubin R. Liver disease and diabetes mellitus. Clin Lab Med 2001;21(1):193-207.

MANUSCRIPT 2:

KEAP1 KNOCKDOWN INCREASES MARKERS OF METABOLIC SYNDROME AFTER LONG-TERM HIGH FAT DIET FEEDING

Vijay R More[1], Jialin Xu[1], Prajakta C Shimpi[1], Clyde Belgrave[2], James P. Luyendyk[3], Masayuki Yamamoto[4], and Angela L Slitt[1]

[1]Department of Biomedical and Pharmaceutical Sciences,
University of Rhode Island, Kingston, RI, 02881; [2]Pathology and Laboratory Medicine, VAMC, Providence [3]Pathobiology and Diagnostic Inv., Michigan State University, East Lansing, MI 48824; [4]Division of Medical Biochemistry, Tohoku University Graduate School of Medicine, Sendai, Japan

---

Manuscript published in *Free Radical Biology and Medicine*, Mar 2013

2.1 Abstract

The Nuclear factor-E2 related factor 2 (Nrf2)-Kelch-like ECH-associated protein 1 (Keap1) pathway upregulates antioxidant and biotransformation enzyme expression to counter cellular oxidative stress. The contribution of Nrf2 to other cellular functions, such as lipid homeostasis is emerging. The present study was conducted to determine how enhanced Nrf2 activity impacts progression of metabolic syndrome with long-term high fat diet (HFD) feeding. C57BL/6 and Keap1-Knockdown (Keap1-KD) mice, which exhibit enhanced Nrf2 activity, were fed a HFD for 24 weeks. Keap1-KD mice had higher body weight and white adipose tissue mass compared to C57BL/6 mice on HFD, along with increased inflammation and lipogenic gene expression. HFD feeding increased hepatic steatosis and inflammation to a greater extent in Keap1-KD mice compared to C57BL/6 mice, which was associated with increased liver Cd36, fatty acid binding protein 4 (Fabp4), and monocyte chemoattractant protein 1 (Mcp1) mRNA expression, as well as, increased acetyl CoA carboxylase 1 (Acc1) and Steroyl CoA desaturase 1 (Scd1) protein expression. The HFD altered short-term glucose homeostasis to a greater degree in Keap-KD mice compared to C57BL/6 mice, which was accompanied by down regulation of Insulin receptor substrate 1 mRNA expression in skeletal muscle. Together, the results indicate that Keap1 knockdown, on treatment with HFD, increases certain markers of metabolic syndrome.

2.2 Introduction

Metabolic syndrome is described as a cluster of risk factors that increase risk for developing cardiovascular disease [1]. Some of the risk factors include central obesity, atherogenic dyslipidemia (elevated triglycerides and low HDL cholesterol), insulin resistance (with or without glucose intolerance), and a proinflammatory state. In 2003-2009, in an analytic sample that consisted of 3,423 adults, 20 years of age and over, 34% of American adults met the criteria for metabolic syndrome [2].

Nuclear factor E2 related factor 2 (Nrf2) is a basic leucine zipper transcription factor, which regulates basal and inducible expression of multiple antioxidant and biotransformation genes [3]. Kelch-like ECH-associated protein 1 (Keap1) is a cysteine rich protein that binds Nrf2 in the cytosol, and is a critical determinant for Nrf2 nuclear accumulation. Dose-dependent accumulation of Nrf2 in nucleus and increasing Nrf2 target gene expression occurs in Nrf2-knockout, Keap1-knockdown and liver-specific Keap1 knockout mice [4]. The effects of Nrf2 and Keap1 knockout/knockdown are well described in models of liver injury caused by acetaminophen, diquat, cadmium, alcohol, or oxidative stress [5-10]. But the effects are largely undescribed for hyperlipidemia and tissues important to metabolic syndrome, such as adipose tissue and skeletal muscle (SKM).

Central obesity is a major hallmark of metabolic syndrome. Multiple nuclear receptors influence stem cell differentiation to adipocytes and adipocyte maturation. For example, multiple CCAAT-enhancer-binding protein isoforms

(Cebpα and Cebpβ) are required at various stages of adipocyte differentiation [11]. Peroxisome proliferator-activated receptor-gamma (Ppar-γ) is known as a key regulator of fat synthesis, which regulates additional genes that contribute to lipid storage, such as Fatty acid binding protein 4 (Fabp4), Cluster of Differentiation 36 (Cd36, fatty acid translocase), Lipoprotein lipase (Lpl) and steroyl CoA desaturase (Scd1) [12]. Acetyl CoA carboxylase 1 (Acc1) catalyzes formation of malonyl CoA, which is a vital substrate for fatty acid biosynthesis [13]. Malonyl CoA also inhibits β-oxidation of fatty acids. Phosphorylated Acc1 (pAcc1) is an inactive form of Acc1. Fatty acid synthase (Fas) uses precursors like acetyl CoA and malonyl CoA to synthesize long chain saturated fatty acids. Steroyl CoA desaturase 1 (Scd1) catalyzes synthesis of unsaturated fatty acids from saturated fatty acids [13]. Lipoprotein lipase (Lpl) breaks down triglycerides (TG) from lipoproteins to release free fatty acids [14]. In summary, all of the abovementioned enzymes/ enzyme complexes are responsible for fatty acid levels in the tissues as well as serum.

Adipocytes function to not only store fat, but also produce and secrete 'adipocytokines' that include bioactive products such as inflammatory mediators (e.g. Interleukin-6, IL-6; monocyte chemoattractant protein, Mcp1; tumor necrosis factor, Tnf), which are considered to be a cause of insulin resistance and non-alcoholic fatty liver disease [15, 16]. Obesity increases the presence of M1 pro-inflammatory macrophages in adipose tissue, increases

secretion of pro-inflammatory cytokines, and increases M1 hepatic macrophages and inflammation [17].

In adipose tissue, Nrf2 binds to an ARE present in the Ppar-γ promoter to promote adipocyte differentiation [18]. Nrf2 knockout mice were protected against hepatic steatosis induced by high fat diet (HFD) feeding [19], indicating that Nrf2 presence is needed for hepatic lipid accumulation. Huang *et al.* (2010) illustrated that targeted Nrf2 deletion protects against high fat diet induced steatosis through dowregulation of Cd36, Sterol regulatory element binding protein 1c (Srebp-1c), Fas, Ppar-γ expression, and upregulation of Small heterodimeric partner (Shp) -dependent pathways. Moreover, OB-Keap1KD exhibit increased hepatic steatosis compared to OB mice [20]. In contrast, Kay *et al.* (2011) report inverse that NRF2 and SREBP1c are inversely regulated in human livers with steatosis [21]. Because hepatic steatosis is a manifestation of metabolic syndrome, better understanding of Nrf2 function in hepatic lipid accumulation in the face of dyslipidemia is needed.

The study herein describes the effect of chronic HFD-feeding on markers of metabolic syndrome including 1) WAT mass and hepatic steatosis, 2) glucose clearance, and 3) WAT and liver inflammation in C57BL/6 and Keap1-knockdown mice. Overall, Keap1-KD mice exhibited increased markers of metabolic syndrome with long-term HFD feeding.

2.3 Materials and methods

2.3.1 Animals. Mice with Keap1 knockdown (Keap1-KD), congenic to C57BL/6 background were generously shared by Dr. Curtis Klaassen (Kansas University Medical Center, Kansas City, KS) and Dr. Masayuki Yamamoto (Tohoku University Graduate School of Medicine, Sendai, Japan). The mice are described in multiple publications from Yamamoto and Klaassen [22-24]. Male age-matched C57BL/6 and Keap1-KD mice were bred in-house and fed diet containing either 10% kcal fat (LFD, Research Diets Inc, D12450B) or 60% kcal fat (HFD, Research Diets Inc, D12492) starting at wean (3 weeks) (n=4 or 5 per group). Body weights were measured every week starting from six weeks of age (3 weeks on diet). At the age of 27 weeks, blood, liver, SKM, and WAT, and brown adipose tissue were collected. The study herein was reviewed and approved by the University of Rhode Island Institutional Animal Care and Use Committee (IACUC protocol # AN11-11-007) and the number of mice used was based upon required power analysis.

2.3.2 Glucose tolerance test (GTT). The GTT was performed on the mice at 25 weeks of age. Mice were fasted for 8 hours overnight and were administered a bolus dose of glucose solution by oral gavage (1g/kg body weight). The blood glucose levels were recorded at 0, 15, 30, 60, and 120 minutes after glucose administration from tail blood using a Contour® glucometer (Bayer HealthCare LLC, Tarrytown, NY).

2.3.3 Hepatic triglyceride (TG) quantification. Total lipids were extracted from liver tissue by methanol-chloroform extraction according to [25] and TGs were quantified using a kit from Pointe Scientific Inc (Canton, MI) according to manufacturer's protocol.

2.3.4 Hematoxylin and Eosin staining. After harvesting, a small section of liver tissue from the central lobe of the liver, WAT, or brown adipose tissue was stored in formaldehyde for 24 hour and then in 75 % ethanol until further processing for paraffin embedding. Paraffin-embedded tissues were cut to approximately 5 μm sections, and then stained with hematoxylin and eosin.

2.3.5 Oil red O staining. Frozen liver tissues were sectioned (5μM) on Vibratome UltraPro 5000 Cryostat® (GMI Inc., Ramsey, MN). Sections were then fixed in 10% formalin for 5 min and slides were washed in water. Then slides were immersed in 60% isopropanol five times and incubated in Oil red O solution for 15 min. The slides were immersed in fresh 60% isopropanol solution twice and then counter stained with hematoxylin. Excess hematoxylin was removed with a water wash and the slides were covered using Vectamount aqueous solution and coverslips.

2.3.6 Neutrophil staining. Neutrophil staining of paraffin embedded liver and WAT sections was performed as described in [26]. Briefly, 4 μM sections on adhesive slides were dried, de-paraffinized and placed in TBS of pH 7.5 for 5

min. Enzyme Induced Epitope Retrieval (20 minutes in 0.04% Pepsin in 0.2NHCl) followed by subsequent rinses and blocking for endogenous peroxidase using 3% Hydrogen Peroxide/Methanol bath (1:4 ratio) for 20 minutes followed by rinses with water. Pretreatment was followed by blocking with rabbit serum and endogenous Biotin blocking by incubation in Avidin D (Vector) and d-Biotin (SigmaAldrich, St.Louis, MO) for 15 minutes. Slides were then incubated with primary antibodies diluted in normal diluent for 1 hr (Neutrophil- NIMP R14 from Santa Cruz Biotech, CA). Biotinylated secondary antibody incubation was followed by RTU VectaStain Elite ABC Reagent (Vector Laboratories, Burlingame, CA), reaction developed by Nova Red followed by counterstain Gill 2 Hematoxylin (Richard Allen, Kalamazoo, MI). The slides were then rinsed, dried and permanently mounted with Flotex media.

2.3.7 Serum cytokine analysis. Serum Mcp1 levels were measured using Mouse Mcp1 ELISA Max kit (# 432704) from Biolegend (San Diego, CA) according to the manufacturer's protocol.

2.3.8 Total RNA extraction and mRNA quantification. Total RNA from liver, WAT and SKM was isolated by phenol-chloroform extraction using RNA Bee reagent (Tel-Test Inc, Friendswood, TX) according to the manufacturer's protocol. RNA concentration was quantified by absorbance at 260 nm using a spectrophotometer (Nanodrop ND1000, Thermo Fisher Scientific, Waltham,

MA) and the samples were diluted to 1 μg/μL. Formaldehyde–agarose gel electrophoresis followed by UV illumination was used to visualize RNA and confirm integrity. Messenger RNA was quantified by QuantiGene (QGP) Plex 2.0 or 1.0 assay.

For QGP 2.0 assay, all the reagents including capture buffer, magnetic capture beads, preamplifier, amplifier, label probe, diluents, and substrate solution were provided in the kit (Affymetrix, Santa Clara, CA). On day one, 1000ng of RNA was incubated with capture beads and target specific probe set mixture for hybridization for 18-22 hrs. After hybridization, the beads were washed on BioPlex Pro wash station I (BioRad, Hercules CA), using magnetic plate washer. Then beads were hybridized with preamplifier, amplifier and label probe for 1 hr each and with washings in-between with wash buffer. After incubation with label probe, the beads were washed and incubated with streptavidin phycoerythrin (SAPE) for 30 min. The beads were then washed with SAPE washing buffer and re-suspended in it for reading on Bioplex microplate luminometer. The data was processed by BioPlex Manager software 5.0. Target gene expression was normalized to Hprt1 expression.

The QGP 1.0 assay (also referred to as the Branched DNA Signal Amplification assay) procedure has been described in detail elsewhere [27, 28]. All reagents for analysis including lysis buffer, amplifier/label probe diluent and substrate solution were supplied in the QuantiGene 1.0 assay kit (Panomics, Fremont, CA). Oligonucleotides were first dissolved in 10 mM Tris-HCl (pH 8.0) containing 1 mM EDTA and were diluted 1:100 in lysis buffer

before use [29]. On day one, total RNA samples (10 μg, 1 μg/μL) were added to wells containing 50 μL of capture hybridization buffer and 50 μL of diluted probe set. The RNA was allowed to hybridize overnight with probe set at 53°C. On day two, subsequent hybridization steps were followed as mentioned in manufacturer's protocol, and luminescence was measured with a GloRunner™ microplate luminometer interfaced with GloRunner DXL Software (Turner Biosystems, Sunnywale, CA). The luminescence for each well was reported as relative light units (RLU) per 10 μg of total RNA. The raw data was used to plot graphs for mRNA expression.

2.3.9 Total protein extraction and western blotting. About 50mg of liver tissue was homogenized in 1mL RIPA buffer using Dounce homogenizer. The homogenate was centrifuged at 12000 rpm for 10 minutes, and the supernatant was stored at -80°C for future use as a total protein fraction. The extract was quantified for protein content by Lowry assay. Relative protein expression was evaluated by western blot. Fifty microgram of total protein extract pre-mixed with Laemmli was loaded on polyacrylamide gel (4% stacking, 12% resolving), transferred on PVDF membrane, stained with different antibodies. All the primary antibodies were obtained from Cell Signaling Inc (Danvers, MA). The membrane was then incubated with ECL+ (GE Healthcare, Waukesha, WI) and chemiluminescence was exposed to X-ray film. The resulting bands on autoradiography films were evaluated using Quantity One® software from BioRad.

2.3.10 Statistical Analysis. Groups were analyzed by a one-way ANOVA followed by a Duncan's Multiple Range *post hoc* test and planned comparison between C57BL/6 and Keap1-KD groups were performed among HFD groups after performing the one-way ANOVA. Different letters indicate statistically significant difference between the groups ($p<0.05$).

2.4 Results

2.4.1 Effect of Keap1-KD on body, WAT, and liver weight and food consumption with long-term HFD feeding. Figure 1A depicts body weight change over 24 weeks. There was no significant difference in body weight between C57BL/6 and Keap1-KD mice fed the LFD. Keap1-KD mice fed HFD had significantly higher body weight between weeks 17-24, compared to C57BL/6 mice fed HFD. At weeks 8 and 9, the HFD did not increase body weight in Keap1-KD mice as much as C57BL/6 mice. However, around 11th week feeding the HFD, the trends in body weight gain appeared to reverse, with Keap1-KD mice having body weight higher than C57BL/6 mice. Food consumption (Fig. 1B) for the LFD groups stayed within the range of 15-20 g/week per mouse for entire duration of the study. For HFD fed mice, it was noted that food consumption appeared slightly higher in C57BL/6, as compared to Keap1-KD mice throughout the study (no statistical significance). Blood glucose levels of the mice throughout the course of study were observed to remain in the range of 100 to 200 mg/dL, with no significant difference between any of the groups (data not shown).

HFD feeding increased WAT weight (Fig 1C) significantly higher in Keap1-KD compared to C57BL/6 mice. At 24 weeks of feeding the LFD or HFD, Keap1-KD mice also had an increased liver-to- body weight ratio as compared to C57BL/6 mice on the respective diet.

2.4.2 Keap1 knockdown increases liver steatosis with chronic HFD feeding. As depicted in Fig. 2A, the HFD increased lipid accumulation in the liver compared to the LFD. Keap1-KD mice fed the HFD had a higher degree of steatosis compared to C57BL/6 mice, as seen with hematoxylin and eosin staining. Oil red O staining of neutral lipids also revealed that the HFD significantly increased hepatic steatosis, with higher levels being observed in Keap1-KD mice (Fig. 2B). Correspondingly, the HFD increased hepatic triglycerides (Fig. 2C); with significantly higher TG levels being detected in livers of Keap1-KD mice compared to C57BL/6 mice.

2.4.3 Keap1 knockdown increases lipogenic gene and protein expression in liver. Fig. 3A depicts lipogenic gene expression on mRNA level in liver. Ppar-γ and Cd36 mRNA expression increased significantly in Keap1-KD mice as compared to C57BL/6 mice, in both LFD and HFD fed groups. Fabp4 mRNA expression increased in Keap1-KD mice fed HFD compared to C57BL/6 mice. Lpl mRNA expression was higher in C57BL/6 mice fed LFD compared to all other groups, whereas Scd1 expression remained unchanged between all the groups. Fig. 3B and 3C depicts increased mRNA expression of Nrf2 and its target genes, NADPH quinone oxidoreductase (Nqo1) and glutamate cysteine ligase, catalytic subunit (Gclc) in livers and WAT of Keap1-KD mice. Expression of Nrf2 and its target genes was quantified in order to characterize the Keap1-KD model.

Protein expression of similar adipogenic targets also tended to increase livers of Keap1-KD mice fed HFD (Fig. 4). HFD slightly increased Ppar–γ protein expression in Keap1-KD mice, however the change did not reach statistical significance. Phosphorylated acetyl CoA carboxylase 1 (pAcc1), Acc1, and Scd1 protein levels were increased in Keap1-KD mice fed HFD compared to C57BL/6 mice. Fatty acid synthase (Fas) protein expression was equivalent among all groups; however, HFD groups displayed an increasing trend in expression (not statistical), as compared to LFD.

2.4.4 Keap1-KD increases liver and WAT tissue inflammation. Neutrophil staining of paraffin-embedded liver sections revealed increased infiltration in the HFD fed mice, with even more neutrophils in Keap1-KD mice fed HFD (Fig. 5A). Serum levels of Mcp1 tended to increase in Keap1-KD mice fed either LFD or HFD, but this did not achieve statistical significance (Fig. 5B). Quantification of relative pro-inflammatory cytokine mRNA expression in liver tissue supported the histological staining. Mcp1 mRNA expression in liver was higher in Keap1-KD compared to C57BL/6 mice fed HFD (Fig. 5C). Tnf mRNA expression remained constant between C57BL/6 and Keap1-KD mice fed same diet.

Chronic feeding of the HFD caused increased cellularity in WAT (Fig. 6A), which is often associated with presence of neutrophils and macrophages [30]. After chronic HFD feeding, WAT from Keap1 mice had increased cellularity and inflammation compared to C57BL/6 mice, as determined by

histopathological analysis. Messenger RNA levels of proinflammatory macrophage M1-marker Tnf was elevated in WAT of Keap1-KD mice fed HFD as compared to C57BL/6 mice fed HFD (Fig. 6B). Mcp1 and Cd11c mRNA levels were higher in HFD fed groups, but there was no significant difference between the C57BL/6 and Keap1-KD mice.

2.4.5 Keap1-KD alters glucose clearance and insulin signaling protein expression in SKM. After 23 weeks of feeding the LFD or HFD, mice were subjected to a glucose tolerance test (GTT), as a measure of diabetes and insulin resistance. No differences in glucose levels after glucose administration were detected between C57BL/6 or Keap1-KD mice fed the LFD. Mice fed the HFD had higher blood glucose levels compared those fed the LFD. After 15, 30 and 60 min of glucose administration, the blood glucose levels of Keap1-KD mice fed HFD were about 1.5 fold higher compared to C57BL/6 mice fed the HFD (Fig. 7A). Area under the curve (AUC) for GTT also demonstrated that blood glucose levels remained significantly high in Keap1-KD mice fed HFD as compared to C57BL/6 mice fed HFD (Fig. 7B) for the duration of 2 hrs.

In accordance with the GTT, the expression of insulin signaling target insulin receptor substrate 1 (Irs1) was also down regulated in SKM. In HFD fed mice, Keap1-KD mice had decreased mRNA expression of Irs1 compared to C57BL/6 mice (Fig. 7C). However, Glut4 mRNA and protein expression was

similar between all the groups, as determined by QGP 2.0 assay and western blot respectively (Fig. 7C and 7D).

2.5 Discussion

Metabolic syndrome is considered to be a manifestation of obesity, characterized by increased central abdominal mass, dyslipidemia (e.g. increased serum triglycerides), increased hepatic steatosis and markers of systemic inflammation, and dysregulation of glucose tolerance [31]. To date, no study has evaluated the effect of Keap1 knockdown on development of metabolic syndrome. The present study demonstrates that Keap1 knockdown increased some markers of metabolic syndrome after long term HFD feeding. Along with increased body weight and WAT mass, Keap1-KD mice fed a HFD displayed increased hepatic and white adipose markers of inflammation, hepatic steatosis, increased adipose cellularity, and altered glucose homeostasis. Taken together, these data suggest that Keap1 knockdown, and perhaps persistent Nrf2 activation, are associated with increased metabolic syndrome risk with HFD challenge.

The present data indicate that Keap1-KD mice had significantly higher body weight and adipose tissue mass compared to C57BL/6 mice with chronic long-term HFD feeding, which are in line with other published findings. Pi *et al.* described adipose tissue changes in $Nrf2^{-/-}$ mice [18]. The body weight of $Nrf2^{-/-}$ mice was significantly lower than wild type mice fed an *ad libitum* diet. Abdominal fat pad mass, and adipocyte size was also significantly smaller in mice with $Nrf2^{-/-}$ mice. $Nrf2^{-/-}$ mice were also resistant to diet-induced obesity, when fed 41% kCal fat diet for 12 weeks after weaning. Also, adipocytes derived from $Nrf2^{-/-}$ mouse embryonic fibroblasts accumulated less lipids

compared to those derived from $Nrf2^{+/+}$ mouse embryonic fibroblasts [18]. Another study by Huang *et al.* also demonstrated that deletion of Nrf2 ($Nrf2^{-/-}$) in mice resulted in reduced body weight in $Nrf2^{-/-}$ mice fed a HFD for approximately three months. These mice also had lower hepatic TG content when challenged with HFD, compared to $Nrf2^{+/+}$ mice [19]. $Nrf2^{-/-}$ mice displayed better insulin sensitivity, measured by glucose tolerance, as compared to wild type mice fed HFD for 180 days [32]. The data herein also demonstrate that Keap1-KD mice display increased hepatic steatosis compared to C57BL/6 mice. It was observed that the HFD increased hepatic lipid accumulation along with increased lipogenic gene and protein expression (e.g. Fabp4 mRNA, Cd36 mRNA, pAcc1 protein), which was augmented in Keap1-KD mice. This observation is consistent with a report by Huang *et al.*, 2010, which reported decreased hepatic lipid accumulation in livers of $Nrf2^{-/-}$ mice after long term HFD feeding. An interesting change in body weights was noted in the HFD fed groups. Up to about 8-9 weeks of feeding the HFD, C57BL/6 mice appeared to have significantly higher body weight as compared to Keap1-KD mice, which is consistent with our previous observation [33]. However, this difference diminished at about 11 weeks of feeding HFD and then by 19 weeks of HFD feeding, Keap1-KD mice weighed significantly higher than C57BL/6. Food consumption did not significantly differ between genotypes, suggesting the observed increase in metabolic syndrome markers in Keap1-KD mice are related to lipid metabolism and not appetite. Zhang *et al.* recently reported no alterations in body and liver weights in Keap1-KD mice

fed 40% kCal fat diet for 12 weeks [34]. The results herein differ from Zhang *et al*., perhaps because our study used 60% kCal fat diet and was significantly longer in duration. However, our results are consistent with Zhang *et al.* and Xu *et al.*, when duration of feeding is considered. For example, in the present study, body weights were similar between C57BL/6 and Keap1-KD mice after 12 weeks of HFD feeding (15 weeks of age), which is consistent with Zhang *et al*. Also, our group reported that Keap1 knockdown protected against HFD-increased weight gain [33], which on a cursory review seems inconsistent with the present study. Again, when one evaluates the response of Keap1-KD mice with regard to duration on a HFD, the present data are also consistent with Xu *et al.* In Xu *et al.*, HFD feeding started at 9 weeks of age for 5 weeks in duration. In the present study, Keap1-KD mice had lower body weights compared to C57BL/6 mice on the HFD after 5 weeks of feeding, consistent with Xu et al [33]. It appears that short term versus long term HFD in Keap1-KD produce different outcomes with regard to body weight.

In contrast to the present finding, others report that activation of Nrf2 is protective against HFD-induced obesity and steatosis, but this is typically reported in conjunction with pharmacological Nrf2 activating compounds. Chemical activators of Nrf2 including, oltipraz, CDDO-imidazole, and sulforaphane in separate studies protected mice against obesity and steatosis [21, 35, 36]. When administered with oltipraz, HFD feeding did not have obesogenic effects on mice for up to 28 weeks. Body weight, liver weight and adipose tissue weight gain induced by HFD feeding was prevented with

oltipraz co-administration C57BL/6J mice [35]. Similarly, the synthetic triterpenoid CDDO-imidazole also prevented weight gain in mice fed HFD for 3 and 13 weeks [36]. In an experiment with hepatocytes, Nrf2 activator sulforaphane suppressed Liver X receptor (Lxr) dependent steatosis [21]. It is not clear why pharmacological Nrf2 activators impact HFD feeding differently compared to genetic models of Nrf2 manipulation, but perhaps other receptor systems (e.g. Constitutive Androstane Receptor and Pregnane x receptor) might also be activated [24, 37]. One must also consider the absorption, metabolism, and disposition of the chemical inducers being administered in comparison to a genetically manipulated mouse model that has whole body Keap1 knockdown.

The present study also demonstrated that constitutive Nrf2 activation altered glucose homeostasis. As GTT is an indicator of sensitivity of cells to respond to insulin action, ability of pancreas to produce insulin and ability of liver to store glucose, expression of insulin responsive targets in the SKM could partially explain the reason for the insulin intolerance. SKM is one of the major glucose utilizing tissues in the body and Glut4 is a predominant glucose transporter responsible for insulin stimulated glucose uptake in SKM [38]. Keap1-KD mice fed the HFD had unaltered mRNA and total protein expression of Glut4. However, the mRNA expression of Irs1 mRNA, a protein involved in molecular basis for action of insulin [39], was decreased in Keap1-KD mice fed the HFD, supporting data obtained from GTT in Keap1-KD mice. It is possible that glucose uptake in skeletal muscles was not altered in Keap1-

KD mice fed HFD due to total Glut4 protein expression. Glut4 translocation to the membrane or defects in Irs-1 or Akt phosphorylation in response to glucose or insulin could also be potentially considered. The Keap1-KD mice fed HFD demonstrate a disturbance in glucose homeostasis with glucose challenge, which does suggest a potential for development of insulin resistance.

Adipocytes act as endocrine cells, secreting variety of adipocytokines including leptin, adiponectin, as well as interleukins [40]. In genetic and diet-induced obese mouse models, the expression of inflammation and macrophage markers was increased in WAT of obese compared non-obese mice [41]. Inflammation is one of the most critical etiological factors in development of insulin resistance [42, 43]. The current data illustrate that the Keap1-KD mice fed the HFD had increased measures of inflammation in WAT and liver. Both WAT and liver had increased inflammation, as noted by increased cellularity (WAT) and neutrophil staining (NIMP R14, Liver). HFD fed Keap1-KD mice were found to have higher levels of cytokines levels in serum and higher expression of cytokine mRNA in liver, as compared to C57 mice fed HFD. Expression of pro-inflammatory M1 macrophage markers was higher in Keap1-KD mice fed HFD, indicating possible role of long term Nrf2 activation in inflammation.

The reason why increased Nrf2 activation might promote lipogenesis and inflammation with HFD feeding is intriguing. It remains to be determined

whether lipid accumulation preceded inflammation, but it is likely. Nrf2 has been shown to be a positive regulator of the mouse Ppar-γ promoter, increase Ppar-γ expression, and promote adipogenesis [18], with a similar mechanism occurring in liver [33]. Thus, the persistent Nrf2 activation in liver appeared to promote lipid accumulation via upstream Ppar-γ activation. Perhaps an increased biotransformation due increased Nrf2 activity resulted in increased lipids that caused tissue injury and inflammation. The data clearly demonstrate increased inflammation in liver and WAT, yet an underlying mechanism for the increased inflammation remains to be determined.

Along with Nrf2, Keap1 is also implicated to interact with Nrf1 [44]. Nrf1, like Nrf2, also belongs to basic leucine zipper family of transcription factors. It plays a role in combating oxidative stress by increasing glutathione levels [45]. However, a review by Biswas and Chan mentioned that functions of Nrf1 and Nrf2 are not completely redundant [46]. Nrf1 also plays role in regulating inflammatory targets including inducible nitric oxide synthase [46]. Although Keap1 has much lower affinity for Nrf1 compared to Nrf2 [47], it is still possible that Keap1-KD mice would have slightly increased levels of Nrf1. The effect of Nrf1 on obesity/ diabetes is a relatively under-investigated area.

Our results herein are also of relevance to the study of obesogenic compounds, as the Nrf2 pathway is inducible and functional in adipose tissue and skeletal muscle [33] and Nrf2 is activated by multiple environmental

chemicals [48]. Thus, it is of potential interest to better understand whether Nrf2 activation via environmental chemical could intersect with obesogenic or pro-metabolic syndrome effects via environmental chemical exposure [49]. In summary, the data herein demonstrate that Keap1-KD mice, which have Keap1 knocked down and constitutive Nrf2 activation, were susceptible to increased markers of metabolic syndrome, such as diet-induced obesity, hepatic steatosis, and glucose intolerance concomitant with increased in inflammation in liver and adipose tissue, after long-term HFD feeding. Overall, this study suggests that Nrf2 has a role beyond combating oxidative stress and further investigation is needed to better understand Nrf2-Keap1 interactions with chronic HFD challenge.

2.6 References

[1] Haffner, S. M. Relationship of metabolic risk factors and development of cardiovascular disease and diabetes. *Obesity (Silver Spring)* **14 Suppl 3:**121S-127S; 2006.

[2] Ervin, R. B. Prevalence of metabolic syndrome among adults 20 years of age and over, by sex, age, race and ethnicity, and body mass index: United States, 2003-2006. *Natl Health Stat Report***:**1-7; 2009.

[3] Tkachev, V. O.; Menshchikova, E. B.; Zenkov, N. K. Mechanism of the Nrf2/Keap1/ARE signaling system. *Biochemistry (Mosc)* **76:**407-422; 2011.

[4] Wu, K. C.; Cui, J. Y.; Klaassen, C. D. Beneficial role of Nrf2 in regulating NADPH generation and consumption. *Toxicol Sci* **123:**590-600; 2011.

[5] Klaassen, C. D.; Reisman, S. A. Nrf2 the rescue: effects of the antioxidative/electrophilic response on the liver. *Toxicol Appl Pharmacol* **244:**57-65; 2010.

[6] Reisman, S. A.; Buckley, D. B.; Tanaka, Y.; Klaassen, C. D. CDDO-Im protects from acetaminophen hepatotoxicity through induction of Nrf2-dependent genes. *Toxicol Appl Pharmacol* **236:**109-114; 2009.

[7] Lamle, J.; Marhenke, S.; Borlak, J.; von Wasielewski, R.; Eriksson, C. J.; Geffers, R.; Manns, M. P.; Yamamoto, M.; Vogel, A. Nuclear factor-eythroid 2-related factor 2 prevents alcohol-induced fulminant liver injury. *Gastroenterology* **134:**1159-1168; 2008.

[8] Okada, K.; Warabi, E.; Sugimoto, H.; Horie, M.; Tokushige, K.; Ueda, T.; Harada, N.; Taguchi, K.; Hashimoto, E.; Itoh, K.; Ishii, T.; Utsunomiya, H.; Yamamoto, M.; Shoda, J. Nrf2 inhibits hepatic iron accumulation and counteracts oxidative stress-induced liver injury in nutritional steatohepatitis. *J Gastroenterol*; 2012.

[9] Wu, K. C.; Zhang, Y.; Klaassen, C. D. Nrf2 protects against diquat-induced liver and lung injury. *Free Radic Res* **46:**1220-1229; 2012.

[10] Wu, K. C.; Liu, J. J.; Klaassen, C. D. Nrf2 activation prevents cadmium-induced acute liver injury. *Toxicol Appl Pharmacol* **263:**14-20; 2012.

[11] Tang, Q. Q.; Otto, T. C.; Lane, M. D. CCAAT/enhancer-binding protein beta is required for mitotic clonal expansion during adipogenesis. *Proc Natl Acad Sci U S A* **100:**850-855; 2003.

[12] Koppen, A.; Kalkhoven, E. Brown vs white adipocytes: the PPARgamma coregulator story. *FEBS Lett* **584:**3250-3259; 2010.

[13] Horton, J. D.; Goldstein, J. L.; Brown, M. S. SREBPs: activators of the complete program of cholesterol and fatty acid synthesis in the liver. *J Clin Invest* **109:**1125-1131; 2002.

[14] Mead, J. R.; Irvine, S. A.; Ramji, D. P. Lipoprotein lipase: structure, function, regulation, and role in disease. *J Mol Med (Berl)* **80:**753-769; 2002.

[15] Lee, Y. H.; Magkos, F.; Mantzoros, C. S.; Kang, E. S. Effects of leptin and adiponectin on pancreatic beta-cell function. *Metabolism* **60:**1664-1672; 2011.

[16] Chawla, A.; Nguyen, K. D.; Goh, Y. P. Macrophage-mediated inflammation in metabolic disease. *Nat Rev Immunol* **11:**738-749; 2011.

[17] Chinetti-Gbaguidi, G.; Staels, B. Macrophage polarization in metabolic disorders: functions and regulation. *Curr Opin Lipidol* **22:**365-372; 2011.

[18] Pi, J.; Leung, L.; Xue, P.; Wang, W.; Hou, Y.; Liu, D.; Yehuda-Shnaidman, E.; Lee, C.; Lau, J.; Kurtz, T. W.; Chan, J. Y. Deficiency in the Nuclear factor E2-related factor 2 transcription factor results in impaired adipogenesis and protects against diet-induced obesity. *J Biol Chem* **285:**9292-9300; 2010.

[19] Huang, J.; Tabbi-Anneni, I.; Gunda, V.; Wang, L. Transcription factor Nrf2 regulates SHP and lipogenic gene expression in hepatic lipid metabolism. *Am J Physiol Gastrointest Liver Physiol* **299:**G1211-1221; 2010.

[20] Xu, J.; Kulkarni, S. R.; Donepudi, A. C.; More, V. R.; Slitt, A. L. Enhanced Nrf2 Activity Worsens Insulin Resistance, Impairs Lipid Accumulation in Adipose Tissue, and Increases Hepatic Steatosis in Leptin-Deficient Mice. *Diabetes*; 2012.

[21] Kay, H. Y.; Kim, W. D.; Hwang, S. J.; Choi, H. S.; Gilroy, R. K.; Wan, Y. J.; Kim, S. G. Nrf2 Inhibits LXRalpha-Dependent Hepatic Lipogenesis by Competing with FXR for Acetylase Binding. *Antioxid Redox Signal* **15:**2135-2146; 2011.

[22] Reisman, S. A.; Yeager, R. L.; Yamamoto, M.; Klaassen, C. D. Increased Nrf2 activation in livers from Keap1-knockdown mice increases

expression of cytoprotective genes that detoxify electrophiles more than those that detoxify reactive oxygen species. *Toxicol Sci* **108:**35-47; 2009.

[23] Taguchi, K.; Maher, J. M.; Suzuki, T.; Kawatani, Y.; Motohashi, H.; Yamamoto, M. Genetic analysis of cytoprotective functions supported by graded expression of Keap1. *Mol Cell Biol* **30:**3016-3026; 2010.

[24] Yates, M. S.; Tran, Q. T.; Dolan, P. M.; Osburn, W. O.; Shin, S.; McCulloch, C. C.; Silkworth, J. B.; Taguchi, K.; Yamamoto, M.; Williams, C. R.; Liby, K. T.; Sporn, M. B.; Sutter, T. R.; Kensler, T. W. Genetic versus chemoprotective activation of Nrf2 signaling: overlapping yet distinct gene expression profiles between Keap1 knockout and triterpenoid-treated mice. *Carcinogenesis* **30:**1024-1031; 2009.

[25] Xu, J.; Kulkarni, S. R.; Li, L.; Slitt, A. L. UDP-glucuronosyltransferase expression in mouse liver is increased in obesity- and fasting-induced steatosis. *Drug Metab Dispos* **40:**259-266; 2012.

[26] Kassel, K. M.; Sullivan, B. P.; Cui, W.; Copple, B. L.; Luyendyk, J. P. Therapeutic Administration of the Direct Thrombin Inhibitor Argatroban Reduces Hepatic Inflammation in Mice with Established Fatty Liver Disease. *Am J Pathol*; 2012.

[27] More, V. R.; Slitt, A. L. Alteration of hepatic but not renal transporter expression in diet-induced obese mice. *Drug Metab Dispos* **39:**992-999; 2011.

[28] More, V. R.; Wen, X.; Thomas, P. E.; Aleksunes, L. M.; Slitt, A. L. Severe diabetes and leptin resistance cause differential hepatic and renal transporter expression in mice. *Comp Hepatol* **11:**1; 2012.

[29] Hartley, D. P.; Klaassen, C. D. Detection of chemical-induced differential expression of rat hepatic cytochrome P450 mRNA transcripts using branched DNA signal amplification technology. *Drug Metab Dispos* **28:**608-616; 2000.

[30] Weisberg, S. P.; McCann, D.; Desai, M.; Rosenbaum, M.; Leibel, R. L.; Ferrante, A. W., Jr. Obesity is associated with macrophage accumulation in adipose tissue. *J Clin Invest* **112:**1796-1808; 2003.

[31] Kahn, S. E.; Hull, R. L.; Utzschneider, K. M. Mechanisms linking obesity to insulin resistance and type 2 diabetes. *Nature* **444:**840-846; 2006.

[32] Chartoumpekis, D. V.; Ziros, P. G.; Psyrogiannis, A. I.; Papavassiliou, A. G.; Kyriazopoulou, V. E.; Sykiotis, G. P.; Habeos, I. G. Nrf2 Represses FGF21 During Long-Term High-Fat Diet-Induced Obesity in Mice. *Diabetes* **60:**2465-2473; 2011.

[33] Xu, J.; Kulkarni, S.; Donepudi, A.; More, V. R.; Slitt, A. L. Enhanced Nrf2 activity worsens insulin resistance, impairs lipid accumulation in adipose tissue, and increases hepatic steatosis in leptin-deficient mice. *Diabetes* **61:**1-11; 2012.

[34] Zhang, Y. K.; Wu, K. C.; Liu, J.; Klaassen, C. D. Nrf2 deficiency improves glucose tolerance in mice fed a high-fat diet. *Toxicol Appl Pharmacol* **264:**305-314; 2012.

[35] Yu, Z.; Shao, W.; Chiang, Y.; Foltz, W.; Zhang, Z.; Ling, W.; Fantus, I. G.; Jin, T. Oltipraz upregulates the nuclear factor (erythroid-derived 2)-like 2 [corrected](NRF2) antioxidant system and prevents insulin resistance and

obesity induced by a high-fat diet in C57BL/6J mice. *Diabetologia* **54:**922-934; 2011.

[36] Shin, S.; Wakabayashi, J.; Yates, M. S.; Wakabayashi, N.; Dolan, P. M.; Aja, S.; Liby, K. T.; Sporn, M. B.; Yamamoto, M.; Kensler, T. W. Role of Nrf2 in prevention of high-fat diet-induced obesity by synthetic triterpenoid CDDO-imidazolide. *Eur J Pharmacol* **620:**138-144; 2009.

[37] Piton, A.; Rauch, C.; Langouet, S.; Guillouzo, A.; Morel, F. Involvement of pregnane X receptor in the regulation of CYP2B6 gene expression by oltipraz in human hepatocytes. *Toxicol In Vitro* **24:**452-459; 2010.

[38] Zorzano, A.; Palacin, M.; Guma, A. Mechanisms regulating GLUT4 glucose transporter expression and glucose transport in skeletal muscle. *Acta Physiol Scand* **183:**43-58; 2005.

[39] Sun, X. J.; Rothenberg, P.; Kahn, C. R.; Backer, J. M.; Araki, E.; Wilden, P. A.; Cahill, D. A.; Goldstein, B. J.; White, M. F. Structure of the insulin receptor substrate IRS-1 defines a unique signal transduction protein. *Nature* **352:**73-77; 1991.

[40] Halberg, N.; Wernstedt-Asterholm, I.; Scherer, P. E. The adipocyte as an endocrine cell. *Endocrinol Metab Clin North Am* **37:**753-768, x-xi; 2008.

[41] Xu, H.; Barnes, G. T.; Yang, Q.; Tan, G.; Yang, D.; Chou, C. J.; Sole, J.; Nichols, A.; Ross, J. S.; Tartaglia, L. A.; Chen, H. Chronic inflammation in fat plays a crucial role in the development of obesity-related insulin resistance. *J Clin Invest* **112:**1821-1830; 2003.

[42] Greenfield, J. R.; Campbell, L. V. Relationship between inflammation, insulin resistance and type 2 diabetes: 'cause or effect'? *Curr Diabetes Rev* **2:**195-211; 2006.

[43] Iozzo, P. Viewpoints on the way to the consensus session: where does insulin resistance start? The adipose tissue. *Diabetes Care* **32 Suppl 2:**S168-173; 2009.

[44] Zhao, R.; Hou, Y.; Zhang, Q.; Woods, C. G.; Xue, P.; Fu, J.; Yarborough, K.; Guan, D.; Andersen, M. E.; Pi, J. Cross-regulations among NRFs and KEAP1 and effects of their silencing on arsenic-induced antioxidant response and cytotoxicity in human keratinocytes. *Environ Health Perspect* **120:**583-589; 2012.

[45] Kwong, M.; Kan, Y. W.; Chan, J. Y. The CNC basic leucine zipper factor, Nrf1, is essential for cell survival in response to oxidative stress-inducing agents. Role for Nrf1 in gamma-gcs(l) and gss expression in mouse fibroblasts. *J Biol Chem* **274:**37491-37498; 1999.

[46] Biswas, M.; Chan, J. Y. Role of Nrf1 in antioxidant response element-mediated gene expression and beyond. *Toxicol Appl Pharmacol* **244:**16-20; 2010.

[47] Kobayashi, A.; Ohta, T.; Yamamoto, M. Unique function of the Nrf2-Keap1 pathway in the inducible expression of antioxidant and detoxifying enzymes. *Methods Enzymol* **378:**273-286; 2004.

[48] Chandler, K. J.; Barrier, M.; Jeffay, S.; Nichols, H. P.; Kleinstreuer, N. C.; Singh, A. V.; Reif, D. M.; Sipes, N. S.; Judson, R. S.; Dix, D. J.; Kavlock,

R.; Hunter, E. S., 3rd; Knudsen, T. B. Evaluation of 309 environmental chemicals using a mouse embryonic stem cell adherent cell differentiation and cytotoxicity assay. *PLoS One* **6:**e18540; 2011.

[49] Marmugi, A.; Ducheix, S.; Lasserre, F.; Polizzi, A.; Paris, A.; Priymenko, N.; Bertrand-Michel, J.; Pineau, T.; Guillou, H.; Martin, P. G.; Mselli-Lakhal, L. Low doses of bisphenol A induce gene expression related to lipid synthesis and trigger triglyceride accumulation in adult mouse liver. *Hepatology* **55:**395-407; 2012.

2.7 Figure legends

Figure 1. Body, liver and WAT weight and adipocyte size of C57BL/6 and Keap1-KD mice fed a 10% kCal low fat diet (LFD) or 60% kCal high fat diet (HFD). A) Body weights (starting from age 6 weeks) and **B)** food consumption of C57BL/6 (C57) and Keap1-KD mice fed a LFD or HFD from weaning age to 27 weeks (starting at age 6 weeks). **C)** Abdominal adipose tissue weight and liver to body weight ratio. Differences between the groups were analyzed by a one-way ANOVA followed by a Duncan's post hoc test. Different letters indicate statistically significant difference between the groups ($p<0.05$). For example, letter "a" is significantly different from "b", but not different from "a". Also, "a" is significantly different from "b,c" but not different from "a,b".

Figure 2. Hepatic lipid accumulation and triglyceride (TG) content in C57BL/6 (C57) and Keap1-KD mice fed a 10% kCal low fat diet (LFD) or 60% kCal high fat diet (HFD). A) Hematoxylin and eosin staining of formaldehyde fixed paraffin embedded liver tissues (200X magnification). **B)** Oil red O staining of liver sections. Frozen liver tissues were sectioned in 5μm sections, stained with Oil red O, and counter stained with hematoxylin (200X magnification). **C)** Hepatic TG content. Lipids were extracted using a methanol-chloroform based protocol and the resulting TG content was assayed using kit from Pointe Scientific (Canton, MI). Differences between the groups were analyzed by a one-way ANOVA followed by a Duncan's post hoc

test. Different letters indicate statistically significant difference between the groups ($p<0.05$).

Figure 3. Lipogenic, Nrf2, and Nrf2 target gene expression in livers and white adipose tissue (WAT) of C57BL/6 (C57) and Keap1-KD mice fed a 10% kCal low fat diet (LFD) or 60% kCal high fat diet (HFD). Total RNA was extracted from the livers by phenol-chloroform extraction and mRNA was quantified using Quantigene Plex 2.0 or Branched DNA Signal Amplification assay (Affymetrix, Santa Clara, CA). **A)** Peroxisome proliferator activated receptor γ (Ppar-γ), Steroyl CoA desaturase (Scd1), Fatty acid binding protein 4 (Fabp4), Lipoprotein lipase (Lpl), and Cluster of differentiation (Cd36) mRNA expression. **B)** Nrf2, NADPH:quinone oxidoreductase (Nqo1), glutamate cysteine ligase (Gclc) mRNA expression in liver. **C)** Nrf2 and Nqo1 mRNA expression in WAT. Differences between the groups were analyzed by a one-way ANOVA followed by a Duncan's post hoc test. Different letters indicate statistically significant difference between the groups ($p<0.05$). For example, letter "a" is significantly different from "b", but not different from "a". Also, "a" is significantly different from "b,c" but not different from "a,b".

Figure 4. Protein expression of lipogenic enzymes in livers of C57BL/6 (C57) and Keap1-KD mice fed a 10% kCal low fat diet (LFD) or 60% kCal high fat diet (HFD). A) Western blots for lipogenic enzymes in liver. Total protein extracts were separated on polyacrylamide gel, immunoblotted, and

chemiluminescence was captured on X-ray films. **B)** Western blot quantification. The resulting blots obtained were evaluated using Quantity One® software (Biorad, Hercules, CA) and band density is plotted as percent of C57BL/6 fed LFD. Differences between the groups were analyzed by a one-way ANOVA followed by a Duncan's post hoc test. Different letters indicate statistically significant difference between the groups ($p<0.05$).

Figure 5. Inflammatory markers in liver and serum of C57BL/6 (C57) and Keap1-KD mice fed a 10% kCal low fat diet (LFD) or 60% kCal high fat diet (HFD). A) Neutrophil (NIMP R14) staining of paraffin embedded liver sections. Images displayed in 200X magnification. **B)** Serum cytokine Monocyte chemoattractant protein 1 (Mcp1) levels **C)** mRNA expression of inflammatory cytokine markers Mcp1, Tumor necrosis factor (Tnf) and Cd11c in liver. Total RNA was extracted from liver tissue by phenol-chloroform extraction and mRNA was quantified using Quantigene Plex 2.0 assay (Affymetrix, Santa Clara, CA). For statistical significance, groups were compared by one-way ANOVA followed by a Duncan's post hoc test. Different letters indicate statistically significant difference between the groups ($p<0.05$).

Figure 6. White adipose tissue (WAT) cellularity and inflammation in C57BL/6 (C57) and Keap1-KD mice fed a 10% kCal low fat diet (LFD) or 60% kCal high fat diet (HFD). A) Hematoxylin and eosin stained sections of paraffin embedded WAT. Images displayed in 200X magnification. **B)**

Messenger RNA expression of proinflammatory macrophage markers monocyte chemoattractant protein 1 (Mcp1), tumor necrosis factor (Tnf) and Cd11c in WAT. Differences between the groups were analyzed by a one-way ANOVA followed by a Duncan's post hoc test. Different letters indicate statistically significant difference between the groups ($p<0.05$).

Figure 7. Glucose tolerance test (GTT) and expression of insulin signaling molecules in skeletal muscle (SKM) of C57BL/6 (C57) and Keap1-KD mice fed a 10% kCal low fat diet (LFD) or 60% kCal high fat diet (HFD). A) GTT after 23 weeks of LFD or HFD treatment. Mice were fasted overnight and challenged with an oral glucose bolus (1g/kg). Blood glucose levels were recorded at 0, 15, 30, 60, and 120-minute time points using Contour® glucose meter (Bayer HealthCare LLC, Tarrytown, NY). *Represents statistically significant difference of glucose levels between C57BL/6 and Keap1-KD mice fed same diet. **B)** Area under the curve (AUC) plotted for the GTT. **C)** Messenger RNA expression of insulin receptor substrate 1 (Irs1) and glucose transporter Glut4 in SKM. Total RNA was extracted from liver tissue by phenol-chloroform extraction and mRNA was quantified using Quantigene Plex 2.0 assay (Affymetrix, Santa Clara, CA). For parts Differences between the groups were analyzed by a one-way ANOVA followed by a Duncan's post hoc test. Different letters indicate statistically significant difference between the groups ($p<0.05$). For example, letter "a" is significantly different from "b", but not different from "a". Also, "a" is

significantly different from “b,c” but not different from “a,b”. **D)** Protein expression of Glut4 from skeletal muscle of C57BL/6 and Keap1-KD mice fed LFD and HFD by western blot (n=2 per group).

2.8 Figures

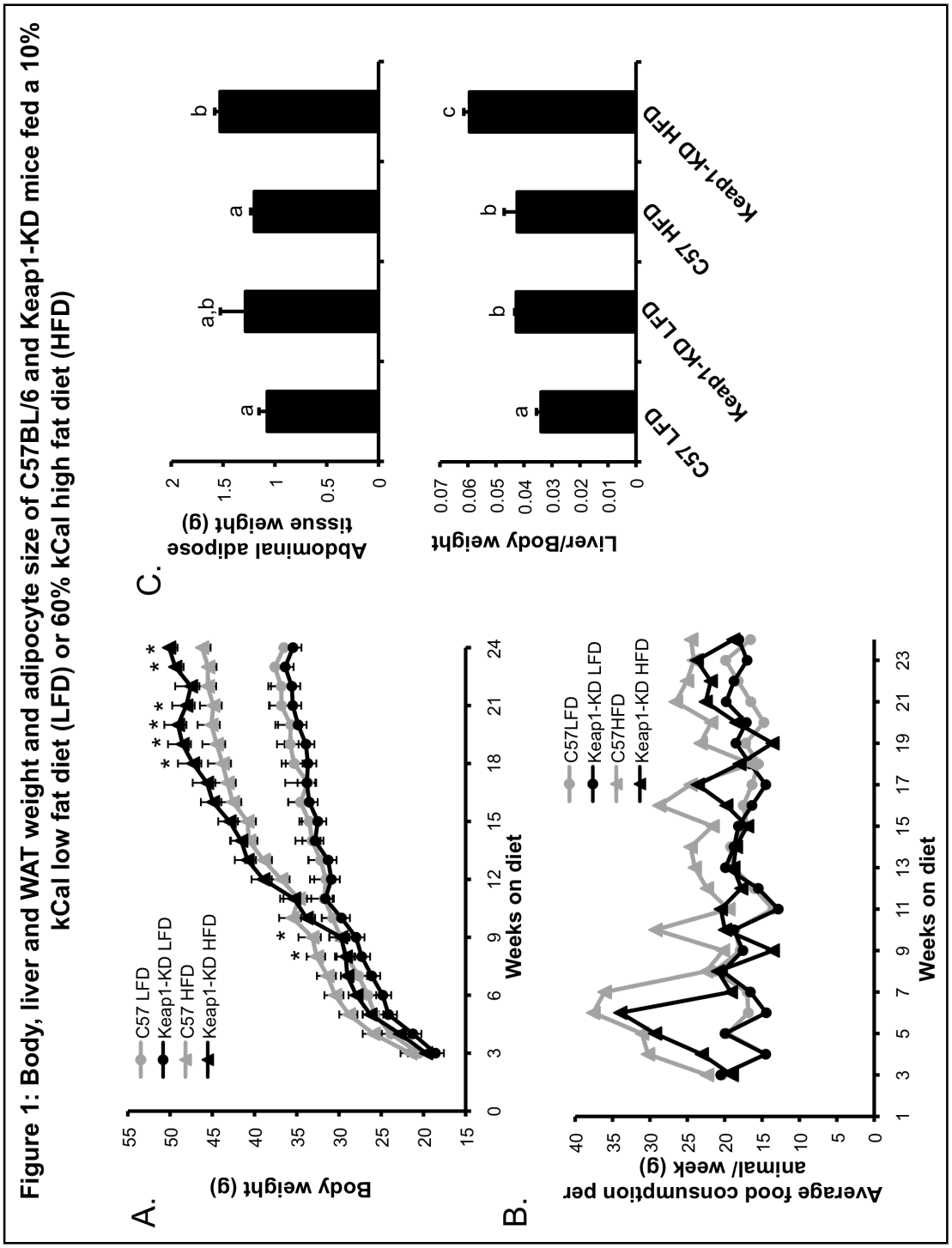
Figure 1: Body, liver and WAT weight and adipocyte size of C57BL/6 and Keap1-KD mice fed a 10% kCal low fat diet (LFD) or 60% kCal high fat diet (HFD)
A.
Body weight (g)
C57 LFD
Keap1-KD LFD
C57 HFD
Keap1-KD HFD
Weeks on diet
B.
Average food consumption per animal/ week (g)
C57LFD
Keap1-KD LFD
C57HFD
Keap1-KD HFD
Weeks on diet
C.
Abdominal adipose tissue weight (g)
Liver/Body weight
C57 LFD
Keap1-KD LFD
C57 HFD
Keap1-KD HFD

Figure 2: Hepatic lipid accumulation and triglyceride (TG) content in C57BL/6 (C57) and Keap1-KD mice fed a 10% kCal low fat diet (LFD) or 60% kCal high fat diet (HFD)

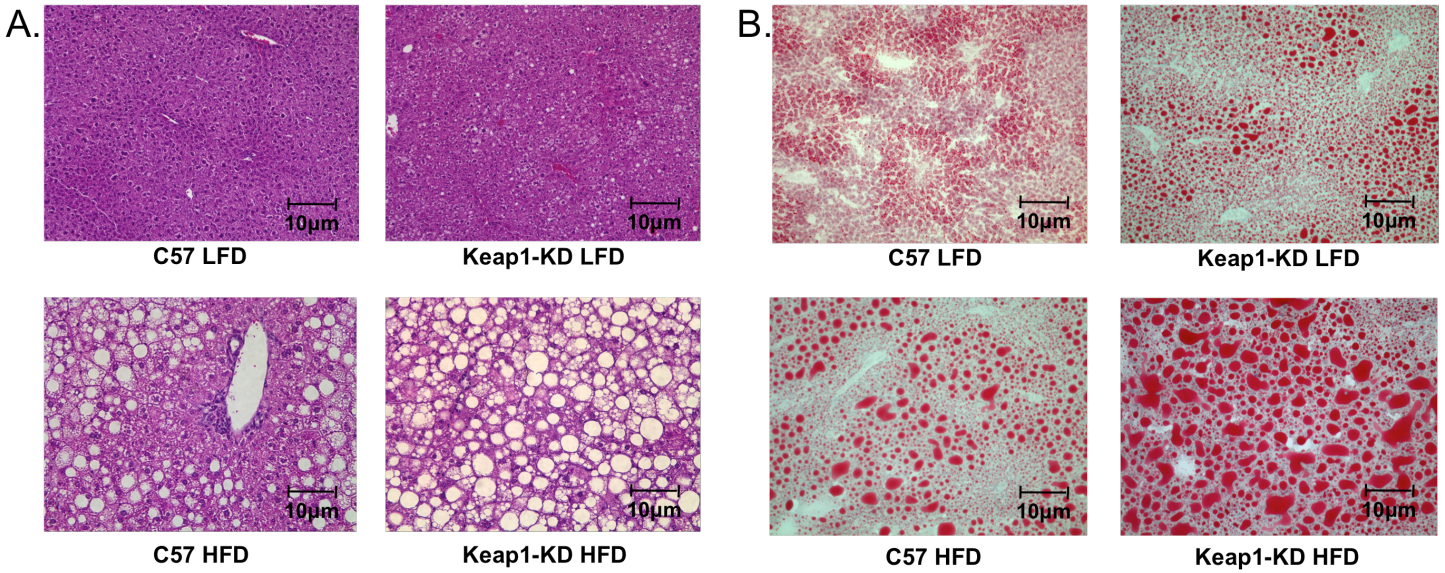

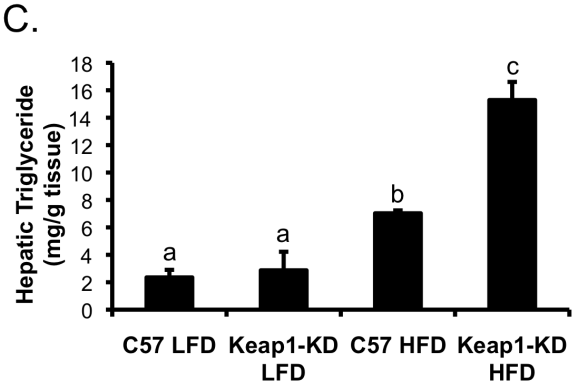

Figure 3. Lipogenic, Nrf2, and Nrf2 target gene expression in livers and white adipose tissue (WAT) of C57BL/6 (C57) and Keap1-KD mice fed a 10% kCal low fat diet (LFD) or 60% kCal high fat diet (HFD)

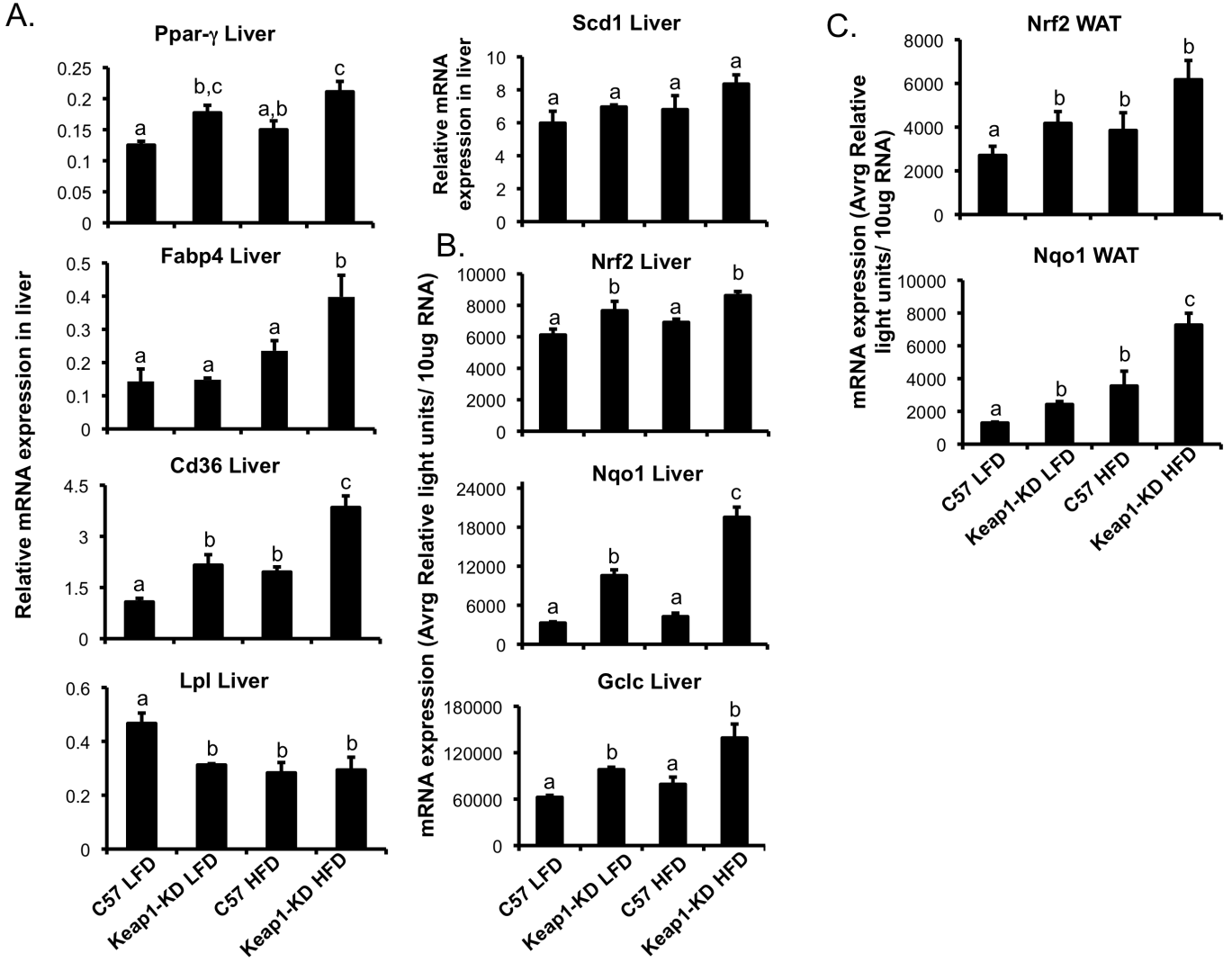

Figure 4: Protein expression of lipogenic enzymes in livers of C57BL/6 (C57) and Keap1-KD mice fed a 10% kCal low fat diet (LFD) or 60% kCal high fat diet (HFD).

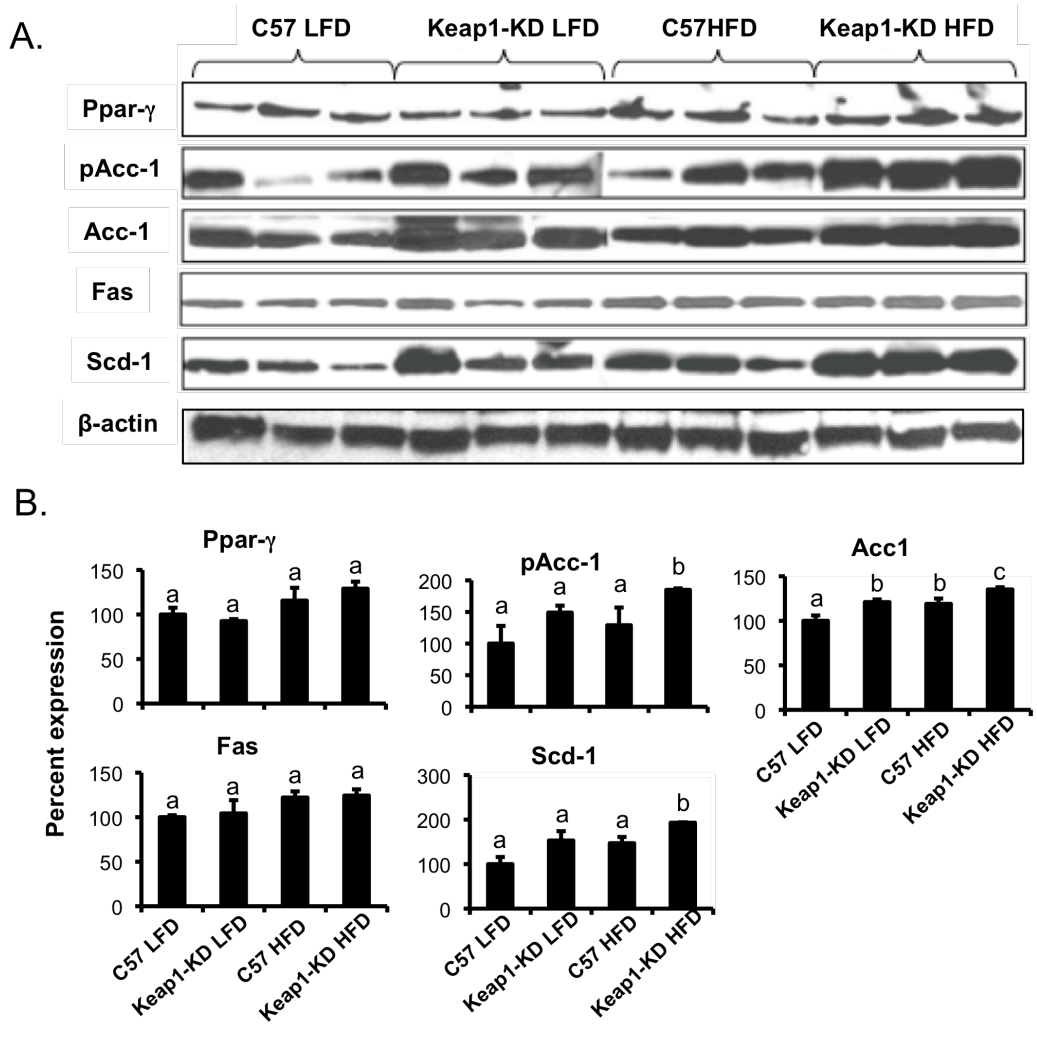

Figure 5: Inflammatory markers in liver and serum of C57BL/6 (C57) and Keap1-KD mice fed a 10% kCal low fat diet (LFD) or 60% kCal high fat diet (HFD)

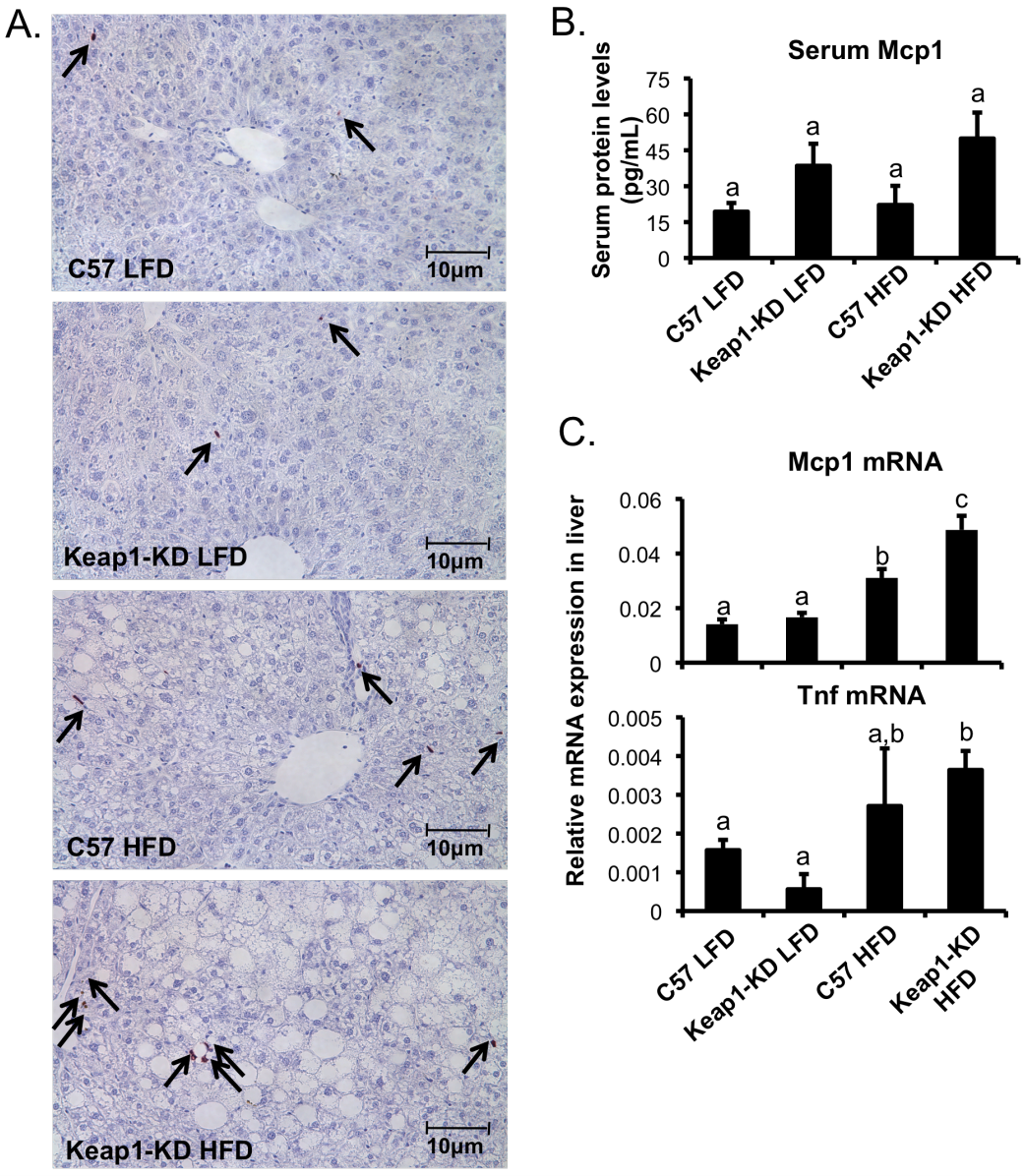

Figure 6: White adipose tissue (WAT) cellularity and inflammation in C57BL/6 (C57) and Keap1-KD mice fed a 10% kCal low fat diet (LFD) or 60% kCal high fat diet (HFD)

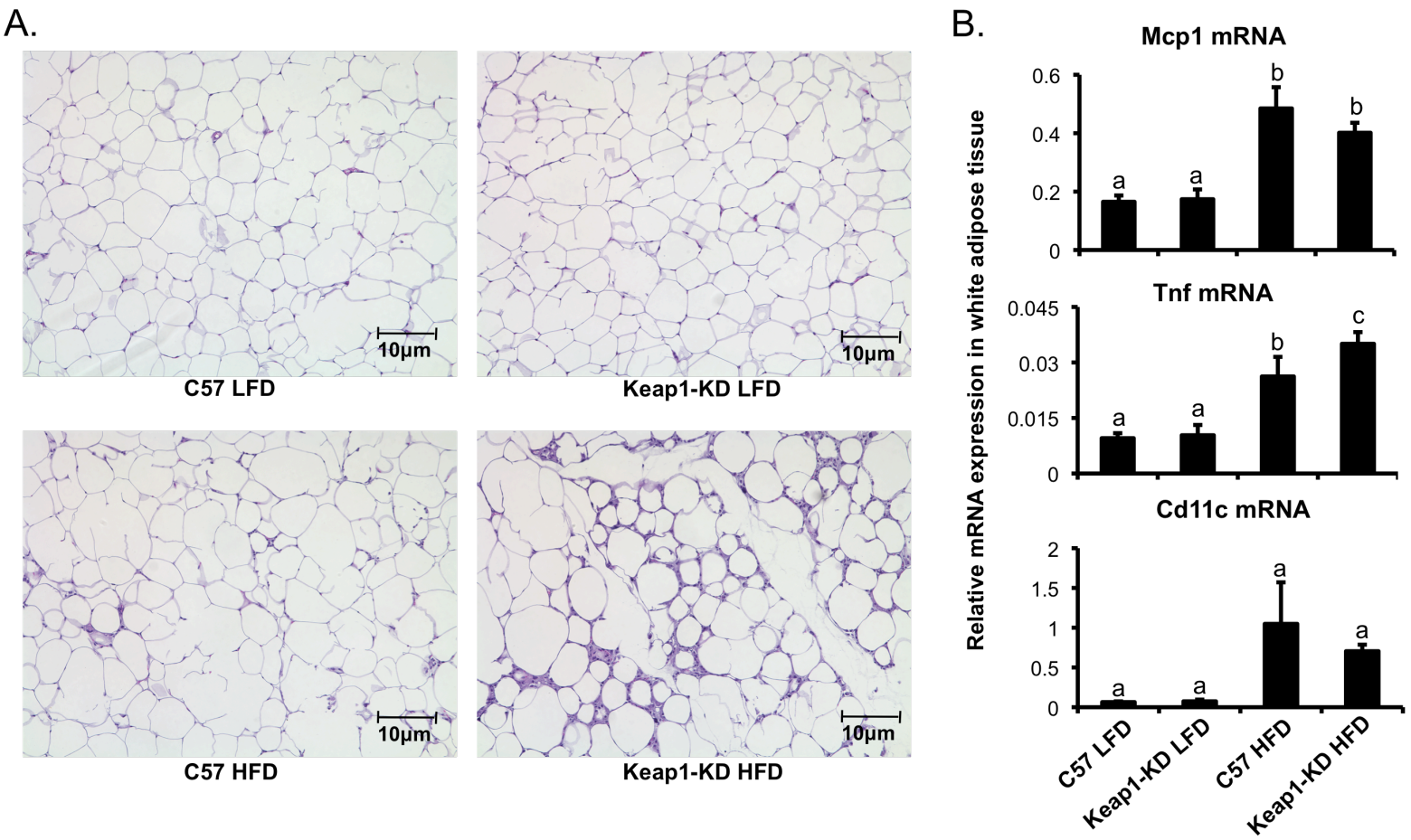

Figure 7: Glucose tolerance test (GTT) and expression of insulin signaling molecules in skeletal muscle (SKM) of C57BL/6 (C57) and Keap1-KD mice fed a 10% kCal low fat diet (LFD) or 60% kCal high fat diet (HFD)

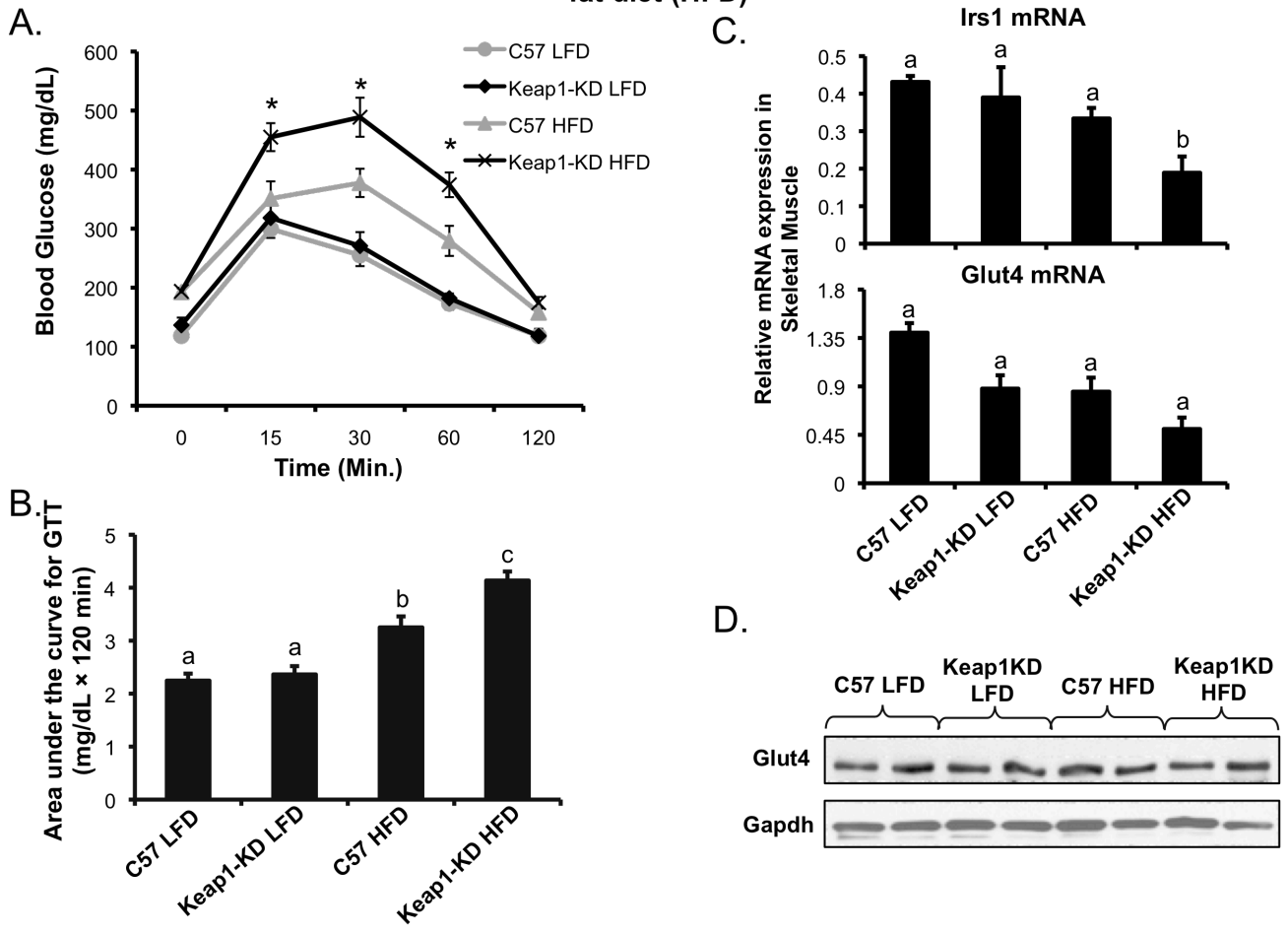

MANUSCRIPT 3:

ALCOHOL CIRRHOSIS ALTERS NUCLEAR RECEPTOR AND DRUG TRANSPORTER EXPRESSION IN HUMAN LIVER

Vijay R. More, Qiuqiong Cheng, Ajay C. Donepudi, David B. Buckley, Zhenqiang James Lu, Nathan J. Cherrington, and Angela L. Slitt

(VM, QC, AD, AS) Biomedical and Pharmaceutical Sciences, College of Pharmacy, University of Rhode Island, Kingston, RI 02881; (DB) Research and Innovation, Xenotech LLC, Lenexa, KS 66219; (ZL) Arizona Statistical Consulting Laboratory, The Bio5 Institute, The University of Arizona, Tucson, AZ 85721; (NC) Department of Pharmacology and Toxicology, College of Pharmacy, University of Arizona, Tucson, AZ 85721

Manuscript published in *Drug Metabolism Disposition* Journal, Mar 2013

3.1 Abstract

Unsafe use of alcohol results in approximately 2.5 million deaths worldwide, with cirrhosis contributing to 16.6% of reported deaths. Serum insulin levels are often elevated in alcoholism, which may result in diabetes; which is why alcoholic liver disease and diabetes often are co-present. Because there is a sizable population that presents with these diseases alone or in combination, the purpose of this study was to determine whether transporter expression in human liver is affected with alcoholic cirrhosis, diabetes, and alcohol cirrhosis co-existing with diabetes. Transporters aid in hepatobiliary excretion of many drugs and toxic chemicals, and can be determinants of drug-induced liver injury. Drug transporter and transcription factor relative mRNA and protein expression in normal, diabetic, cirrhotic and cirrhosis with diabetes human livers were quantified. Cirrhosis significantly increased ABCC4, 5, ABCG2 and SLCO2B1 mRNA expression, and decreased SLCO1B3 mRNA expression in liver. ABCC1, 3-5, ABCG2 protein expression was also upregulated by alcohol cirrhosis. ABCC3-5, and ABCG2 protein expression was also upregulated in diabetic-cirrhosis. Cirrhosis increased NRF2 mRNA expression, whereas it decreased PXR and FXR mRNA expression in comparison to normal livers. Hierarchical cluster analysis indicated that expressions of ABCC2, 3 and 6; SLCO1B1 and 1B3; and ABCC4 and 5 were more closely related in the livers from this cohort. Overall, alcohol cirrhosis altered transporter expression in human liver.

3.2 Introduction

Hepatobiliary excretion is an integral function necessary to excrete bile acids, bilirubin, conjugated hormones, as well as, drugs and chemicals from liver (Klaassen and Aleksunes, 2010). The process of biliary excretion relies upon membrane bound transporters localized to hepatocytes, which extract chemicals from blood and efflux chemicals into bile. The solute carrier organic anion (SLCO) and ATP-Binding Cassette (ABC) transporter families comprise two major families that mediate hepatic uptake and efflux processes.

SLCO transporters are often described as “uptake transporters”, because they are predominantly localized to the sinusoidal membrane and typically extract chemicals from blood into hepatocytes (reviewed by (Klaassen and Aleksunes, 2010)). In humans, SLCO1B1, 1B3, 2B1 and 1A2 have relatively high expression in liver. SLCO1B1, 1B3, and 2B1 transport a diverse range of drugs including benzylpenicillin, statins, and estradiol glucuronide (Klaassen and Aleksunes, 2010). Identification of SNPs in the *SLCO1B1* gene and resulting SLCO1B1 polymorphisms results cause altered disposition of statins (Generaux et al., 2011). Human SLCO mRNA expression is regulated through transcription factor-mediated pathways, such as Liver-X-Receptor (LXR), Farnesoid-X-Receptor (FXR), Constitutive Androstane Receptor (CAR), Pregnane-X-Receptor (PXR) (Svoboda et al., 2011).

The ATP-binding cassette (ABC) transporter superfamily facilitates chemical efflux; and includes Multidrug Resistance Proteins (ABCB), Multidrug Resistance-Associated Proteins (ABCC), Bile Salt-Export Pump (ABCB11), and Breast Cancer Resistance Protein (ABCG2). In liver, ABCC2, ABCG2 and ABCBs are localized to the canalicular membrane and facilitate biliary excretion of chemicals. ABCC1, 3-6 are localized sinusoidally and/or basolaterally, and efflux chemicals from hepatocytes into blood. Similar to SLCOs, human ABCC expression is modulated by transcription factors, such as Nuclear Factor-E2 related factor 2 (NRF2), CAR, PXR, and FXR (Klaassen and Slitt, 2005).

Alterations in transporter expression and function due to hepatic stress have been noted and can have significant implications on the fate of numerous drugs. Hepatic steatosis resulting from obesity and/or diabetes resulted in significant alterations in transporter expression in hepatocytes, as demonstrated in mouse models (Cheng et al., 2008; More and Slitt, 2011; More et al., 2012). As compared to steatosis, cirrhosis is a significant hepatic stress with replacement of normal functional tissue by scar tissue, which is unable to maintain the functions of the liver. According to Center for Disease Control and prevention (CDC), more than 15,000 Americans die every year from alcoholic liver cirrhosis (National Vital Statistics Report, Volume 60, No 3). Other major causes of cirrhosis include chronic viral hepatitis, non-alcoholic steatohepatitis (NASH), and damaged or blocked bile flow (Anand, 1999).

About 30% of cirrhotic patients also suffer from diabetes (Hickman and Macdonald, 2007). Acute, as well as chronic alcohol consumption leads to development of insulin resistance, which can progress to diabetes mellitus (Kim and Kim, 2012). Disruption of normal functions of the liver in cirrhosis may lead to hepatogenous diabetes (Garcia-Compean et al., 2009). Additionally, obesity and diabetes mellitus increase the severity of alcoholic liver disease (Raynard et al., 2002). Owing to interplay between diabetes and cirrhosis, the two conditions often co-present clinically (Baig et al., 2001).

Since many human Phase-I and -II biotransformation enzymes are coordinately regulated by transcription factors that regulate transporter expression, representative cytochrome p450 (CYP), UDP glucuronosyl transferase (UGT), and Nad(p)h:quinone oxidoreductase (NQO1) mRNA expression was also determined. The purpose of this study was to determine whether alcohol cirrhosis alone, or in combination with diabetes, alter transporter expression in intact human liver, as transporters are integral for the hepatobiliary clearance of drugs, bile acids, and bilirubin. Our study has included analysis of livers from subjects who presented with steatosis or diabetes without cirrhosis, as these diseases are sometimes present in alcoholics. Our findings herein illustrate coordinated alterations in the expression of certain SLCO and ABC transporter members in human alcohol cirrhotic liver tissues.

3.3 Materials and Methods

3.3.1 Human liver tissues. Liver tissues from normal healthy, alcohol cirrhotic, steatotic, and diabetic-cirrhotic (co-existence of alcohol cirrhosis and diabetes) subjects were obtained from Liver Tissue Cell Distribution System (LTCDS), University of Minnesota (Minneapolis, MN). Additional liver lysates in Trizol reagent from normal and diabetic subjects were purchased from Xenotech LLC (Lenexa, KS) and were only analyzed for mRNA expression. The details of subject age, gender and ethnicity are mentioned in table 1. Exemption approval from the University of Rhode Island Institutional Review Board was granted before tissues were procured.

3.3.2 RNA Extraction. Total RNA from liver was isolated by phenol-chloroform extraction using RNA Bee (Tel-Test Inc, Friendswood, TX) according to the manufacturer's protocol. Tissue lysates obtained in Trizol were directly homogenized and subject to chloroform extraction. RNA concentration was quantified by absorbance at 260 nm (Nanodrop ND1000, Thermo Fisher Scientific, Waltham, MA). Agarose gel electrophoresis followed by UV illumination was used to visualize RNA and confirm integrity.

3.3.3 Quantigene Plex 2.0 assay for mRNA quantification. Only samples in which total RNA looked intact and not degraded were subjected to analysis the QuantiGene Plex 2.0 assay (Affymetrix, Santa Clara, CA). However, a benefit to this technology according to the manufacturer is that it allows for detection

of partially degraded mRNA transcripts, which is desirable for RNA isolated from human tissue. The protocol for the assay is described elsewhere (Aleksunes et al., 2009). Briefly, 1.1 µg total RNA was incubated with beads with capture probe, label extender and blocker. On day two, the beads were washed and incubated with amplifier, and subsequently with label. Then incubation with streptavidin containing substrate was used for detection on BioPlex Luminometer.

3.3.4 Tissue fractionation. Approximately 100mg of tissue was homogenized in Sucrose-Tris (ST) buffer (250 mM sucrose, 10 mM Tris-HCl buffer, pH 7.4) and containing protease inhibitor cocktail (2 µg/mL, Sigma-Aldrich, Co, St. Louis, MO). Homogenates were centrifuged at 100,000 xg for 60min at 4°C. The resulting pellet is a typical fraction used to detect transporter expression as described by our previous publications as well as multiple other research groups (Trauner et al., 1997; Aleksunes et al., 2006; Campion et al., 2008; Cheng et al., 2008; Maher et al., 2008). The supernatant was saved as a cytosolic fraction to measure NQO1 and GPX1 protein expression. ST buffer (200 µl) was used to re-suspend the resulting pellet. Nuclear fractions from approximately 100 mg of liver tissue were isolated using a NE-PER nuclear extraction kit (Thermo Scientific, Rockford, IL) according to the manufacturer's instructions. Protein concentration of the membrane fractions was determined using the DC protein assay (Bio-Rad Laboratories, Hercules, CA).

3.3.5 Western blot analysis. Western blots were used to quantify the relative expression of transport proteins in human liver tissues, as described in our previous publication (More and Slitt, 2011; More et al., 2012). Briefly, the membrane/ nuclear extracts were separated on polyacrylamide gel (10% resolving, 4% stacking), transblotted on PVDF membrane, and blocked with 2% non-fat dry milk in phosphate buffered saline with Tween 20 (PBS/T). The membranes were then incubated with specific primary and secondary antibody, and then with ECL+ fluorescence reagent. The blots were then developed on X-ray films; protein bands on the resulting autoradiographs were quantified using Quantity One® software v4.6.3 (Biorad, Hercules, CA). Table 2 provides the antibody source and western blot conditions. OATP1B1 and 1B3 protein expression by Western blot was not determined due to lack of high quality commercially available antibodies.

3.3.6 Statistical analysis. Raw data from mRNA quantification was normalized to housekeeping gene hypoxanthine phosphoribosyl transferase 1 (HPRT1). Log transformed normalized data was more approximately normally distributed as compared with non-transformed data. Within each gene, pairwise comparison of expression between disease groups was tested a one-way ANOVA followed by a Tukey Honestly Significant Difference (HSD) test. Data from protein quantification was plotted as percent expression and analyzed by one-way ANOVA followed by Dunnett's *post hoc* test. Difference

of p≤ 0.05 was considered statistically significant. Asterisks (*) represent a statistical difference (p≤0.05) from normal non-steatotic livers, and dots (●) represent outliers. Hierarchical clustering analysis with Pearson correlation as a similarity measurement was also done to discover potential groups of genes with high correlation.

3.4 Results

3.4.1 Transporter mRNA expression in liver is altered by alcohol cirrhosis and diabetic-cirrhosis. Alcohol cirrhosis altered mRNA expression of some transporters (Fig. 1A). SLCO1B1 mRNA expression was similar among all groups examined. SLCO1B3 mRNA expression was significantly decreased in livers from alcohol cirrhosis patients compared to normal non-steatotic livers. In contrast, SLCO2B1 mRNA expression was increased with alcohol cirrhosis compared to normal non-steatotic livers.

In liver, ABCC transporters are localized to the canalicular (ABCC2 and ABCG2) or sinusoidal membranes (ABCC1, 3-6) of hepatocytes, and mediate organic anion efflux from hepatocytes (Klaassen and Aleksunes, 2010). ABCC1, 4 and 5 mRNA expression was increased in alcohol cirrhotic livers compared to normal non-steatotic livers (Fig. 1B). ABCC2 mRNA expression remained unchanged between the groups compared, whereas ABCG2 expression was increased in livers from subjects with alcohol cirrhosis (Fig. 1B). Diabetic-cirrhosis decreased ABCC3 expression compared to normal non-steatotic livers. ABCC6 mRNA expression was similar among from normal, steatotic, alcohol cirrhotic, diabetic-cirrhotic, and diabetic livers.

3.4.2 Transporter protein expression is altered in livers from subjects with steatosis, alcohol cirrhosis, and diabetic-cirrhosis. Fig. 2 illustrates the effect of steatosis, alcoholic cirrhosis, and diabetic-cirrhosis on transporter protein expression in fractions from intact human liver tissue (representative

blots). Alcoholic cirrhosis and diabetic-cirrhosis increased ABCC1, 3, and 5 protein expression compared to normal non-steatotic livers. ABCC2 protein remained unchanged between all the groups. ABCC4 and ABCG2 protein expression was increased in livers with steatosis, alcohol cirrhosis and diabetic cirrhosis. In contrast to other ABC transporters, ABCC6 protein expression decreased in livers with alcohol cirrhosis and diabetic cirrhosis.

3.4.3 Alcoholic cirrhosis and diabetic-cirrhosis affect transcription factor expression in intact human liver. Studies in recent years have revealed several transcription factor-mediated pathways (e.g. PXR, CAR, and FXR), as well as the antioxidant response (e.g. NRF2), are important mediators of SLCO and ABC transporter regulation in liver (Klaassen and Aleksunes, 2010). Therefore, NRF2, PXR, CAR, and FXR expression was also evaluated and correlated with transporter expression. Fig. 3A depicts the PXR, CAR FXR, and NRF2 mRNA expression in human liver. NRF2 mRNA expression was increased in alcohol cirrhotic and diabetic-cirrhotic livers compared to normal non-steatotic livers. PXR mRNA expression was decreased in livers with diabetic-cirrhosis, as compared to normal livers. CAR mRNA expression remained unchanged between all groups analyzed. FXR mRNA expression was decreased in livers with alcohol cirrhosis and diabetic-cirrhosis.

3.4.4 Alcohol cirrhosis affects phase-I and phase-II drug metabolizing enzymes mRNA expression. Correspondingly, Figure 3B depicts mRNA

expression for representative CYP and UGTs, along with FXR target gene, Small Heterodimer Protein (SHP). UGT1A3 mRNA expression was increased in steatotic livers compared to normal livers. CYP3A4 mRNA expression was increased in livers with steatosis, but similar to normal livers in the other disease conditions. CYP2B6 mRNA expression was decreased in livers with diabetic-cirrhosis compared to normal non-steatotic livers. SHP mRNA expression was similar among all the disease conditions tested in the study. Other CYP and UGT isoforms including CYP2D6, UGT1A1, 1A4 mRNA expressions were also studied, and remained unchanged between the groups (data not shown).

3.4.5 Alcohol cirrhosis increases NRF2, NQO1, and Glutathione Peroxidase protein expression. NRF2 protein expression in liver fractions was correspondingly increased in alcohol cirrhotic and diabetic-cirrhotic livers compared to normal non-steatotic livers (Fig. 3C and 3D). NQO1 and Glutathione Peroxidase 1 (GPX1), enzymes, which are regulated via NRF2, were also quantified at protein level. NQO1 protein expression was increased in steatotic, alcohol cirrhotic and diabetic-cirrhotic livers compared to normal livers, with the most prominent increase present in alcohol cirrhosis. GPX1 protein expression was increased in liver fractions from subjects with alcohol cirrhosis and diabetic-cirrhosis.

3.4.6 Alcohol cirrhosis increases inflammatory cytokine mRNA expression. Fig. 4 demonstrates mRNA expression of inflammatory cytokines tumor necrosis factor α (TNFα), and interleukin 1β (IL1β) in livers. TNFα mRNA expression was increased in both steatosis and alcohol cirrhosis groups, as compared to normal non-steatotic livers. IL1β expression was increased only with steatosis as compared to normal livers.

3.4.7 Hierarchical cluster analysis of transporter and transcription factor mRNA expression. Fig. 5 depicts the correlations between transcription factor and transporter mRNA expression. ABCG2 and SLCO2B1 expression were closely related to CAR expression. Similarly, expression of ABCC4, ABCC5 and NRF2 were closely related. Expression of ABCC2 and PXR were also closely related, and more distantly related to SLCO1B3 and 1B1 expression.

3.5 Discussion

This study demonstrated predominant increased mRNA and protein of efflux transporters, such as ABCG2, ABCC1, 3-5 in intact livers of human subjects with alcohol cirrhosis. Uptake transporter expression was less consistent, with decreased SLCO1B3 and increased SLCO2B1 mRNA expression occurring in livers with alcoholic cirrhosis. Transcription factors that regulate transporter expression were also correspondingly altered. NRF2 mRNA and protein expression was increased in alcoholic cirrhotic livers, whereas FXR mRNA expression was decreased.

Hierarchical cluster analysis of transcription factors and transporters obtained in this study is in agreement with the findings in literature. In rodents as well as in humans, NRF2 is known to regulate expression of efflux transporters ABCC2-5 (Klaassen and Slitt, 2005). In the cluster analysis in the present study, ABCC4 and 5 were expressed together with NRF2. Similarly, SLCO2B1 and CAR were expressed together, as observed in rodents (Cheng et al., 2005). ABCC2 and PXR were also clustered together, as also described (Klaassen and Slitt, 2005). SLCO1B1 and 1B3 are reported to be regulated by same transcription factors hepatocyte nuclear factor (HNF) 1α, aryl hydrocarbon receptor (AHR) and CAR (Klaassen and Aleksunes, 2010), and were clustered together in present data. CAR and PXR activation have been shown to increase ABCC2 and 3 expression in hepatocytes (Teng and Piquette-Miller, 2005), indicating that these two transporters also have significant correlation in expression. CAR is known to regulate ABCC2, 3 as

well as SLCO1B1, indicating significant correlation in the expression of these three transporters.

Transporter expression in human livers with alcohol cirrhosis has not been characterized comprehensively before this study. Rodent models for alcohol-induced liver disease display steatosis and some degree of fibrosis, but no model fully progresses to the human level of cirrhotic liver (Lieber et al., 1965; Tsukamoto et al., 1986). Previous studies with hepatic transporter expression are with small sample size and/or different liver pathologies like hepatitis C, hepatocellular carcinoma, NASH, or from non-diseased human livers (Nishimura and Naito, 2005; Hilgendorf et al., 2007; Ogasawara et al., 2010; Doi et al., 2011). Hepatitis C virus-related cirrhosis was reported to increase mRNA and protein expression of ABCC4 in human livers (Ogasawara et al., 2010), which is consistent with alcohol cirrhosis and diabetic-cirrhosis findings from the present study. Another study reported a patient having lowered SLCO1B3 expression in hepatocellular carcinoma nodule (Doi et al., 2011), which is consistent with the present data that illustrate decreased SLCO1B3 mRNA expression in alcohol cirrhosis too. Efflux transporter expression in human livers with primary billiary cirrhosis (PBC) was also similar to alcohol cirrhotic livers in this study (Zollner et al., 2003). ABCC3 protein expression was increased in PBC and alcohol cirrhosis. Uptake transporter SLCO1B1, however, remained unchanged with alcohol cirrhosis, but went down with PBC (Zollner et al., 2003). Fatty and non-fatty NASH also enhanced the mRNA and protein expression of ABCC1, 4 and 5 in human livers (Hardwick et al., 2011).

As other models of liver injury (e.g. acetaminophen, carbon tetrachloride, cholestasis) also increase efflux transporter expression, we acknowledge that the observation was anticipated. However, because alcohol cirrhosis plagues about 20% of the alcoholic people worldwide, knowing whether aberrant transporter and nuclear receptor expression is present in liver is of toxicological significance because it can provide mechanistic understanding of drug-induced liver injury or altered drug efficacy in patients with alcoholic liver disease.

Transporters facilitate absorption, distribution and elimination of xenobiotics, as well as endobiotics such as bile acids, cholesterol, and conjugated hormones (e.g. estrogens and thyroid hormones) (Klaassen and Aleksunes, 2010). Alterations in the transporter expression or polymorphisms have been associated with alterations in disposition and adverse effects/ protection against adverse effects of certain xenobiotics. Simvastatin-induced myopathy, which is concentration dependent side effect, was found associated with SLCO1B1 polymorphism in human subjects (reviewed by (Niemi et al., 2011)). In another study with methotrexate, it was observed that variants of SLCO1B1 were associated with increased clearance and gastrointestinal toxicity as a side effect in children with acute lymphoblastic leukemia (Trevino et al., 2009). In a different study, mice with increased Abcc3 and 4 expression in liver had enhanced metabolite excretion and were protected against acetaminophen induced hepatocyte injury (Slitt et al., 2003; Aleksunes et al., 2008) and mice

lacking Abcc2, 3 and Abcg2 demonstrate mild hepatotoxicity when administered diclofenac (Lagas et al., 2010). The present study illustrates that intact livers from subjects with alcohol cirrhosis have alterations in major drug transporter mRNA and protein expression in liver. As transporters play a vital role in drug disposition, the findings in this study imply that subjects with above mentioned disease conditions need a consideration while administering drugs that form glucuronide, which are pharmacologically active.

With progression of NAFLD, the expression of Nrf2 and its target genes increases, as determined by immunohistochemistry in human livers (Hardwick et al., 2010). Alcohol-induced oxidative stress also activates Nrf2 in human hepatocytes (Nussler et al., 2010). Alcohol induces lipid deposition in liver; and metabolism of fatty acids as well as ethanol causes generation of oxidative stress in liver (Syn et al., 2009). Alcohol cirrhotic livers in the current study also displayed increased Nrf2 protein levels in nuclear fractions, which is likely a response to increased oxidative stress in the alcoholic liver. PXR is indicated in therapeutic applications against inflammatory liver diseases. PXR activation by pregnenolone-16-alpha carbonitrile leads to decreased carbon tetrachloride induced fibrogenesis in rats (Marek et al., 2005). The decreased PXR expression may be an indicator that PXR deficiency correlates with increased risk for liver disease. FXR regulates bile acid homeostasis, TG and cholesterol metabolism, glucose homeostasis and fibrogenesis in liver (reviewed by (Fuchs, 2012)). FXR activation by bile acids induces PPARα expression, and this increases β-oxidation of fatty acids (Pineda Torra et al.,

2003). Thus FXR activation may protect liver from fat deposition in both alcoholic, as well as, non-alcoholic liver diseases. In present study, FXR mRNA expression was decreased in alcohol cirrhosis, suggesting that FXR suppression might occur during alcoholic liver disease, which could be a mechanism for alcoholic liver injury. Inflammation could be a possible factor contributing to the alterations in nuclear receptors analyzed in this study. Lipopolysaccharide treatment of mice resulted in decreased PXR signaling and target gene expression in mice (Moriya et al., 2012). Similarly, treatment of Huh7 cells with inflammatory cytokines TNFα and IL6 resulted in marked decrease in FXR target transporter BSEP (Chen et al., 2012). As disease progression of cirrhosis involves increase in inflammation, decreased mRNA expression of PXR/ FXR in alcohol cirrhosis/ diabetic cirrhosis could possibly be explained. Further studies are necessary in order to elucidate why PXR and FXR expression is decreased in alcohol cirrhosis, and whether the decreased expression contributes to the development of alcohol cirrhosis.

Elbekai et. al., in 2004 reported that certain Phase-I biotransformation enzyme expression was altered expression in livers of cirrhotic subjects. CYP1A and CYP3A showed reduced expression with cirrhosis, whereas CYP2C, 2A and 2B remained unaltered (Elbekai et al., 2004). The present data display little or no change in CYP isoform mRNA expression. Similarly, glucuronidation activity in liver is reported to be unaltered with cirrhosis (Elbekai et al., 2004). The present study had results consistent with this observation – UGT1A1, 1A3, 1A4, and 2B7 expression was remained unchanged between normal and

alcohol cirrhotic livers, although it should be noted that UGT1A3 was decreased in diabetic-cirrhosis livers and UGT2B7 was decreased in diabetic livers.

In summary, we demonstrate that alcohol cirrhosis significantly alters transporter expression in human liver, most notably altering ABCC3, ABCC4, and, ABCC5, which was associated with altered NRF2, CAR, and FXR mRNA expression. Significant correlations between transporter and nuclear receptor expression were observed in the cohort of livers analyzed. Overall, the data herein illustrate alterations in hepatic transporter expression in the alcohol cirrhotic liver that correlates to changes in nuclear receptor expression. Alterations in nuclear receptor and drug transporter expression in alcoholic liver should be given consideration when evaluating altered drug toxicities.

3.6 References

Aleksunes LM, Campion SN, Goedken MJ, and Manautou JE (2008) Acquired resistance to acetaminophen hepatotoxicity is associated with induction of multidrug resistance-associated protein 4 (Mrp4) in proliferating hepatocytes. *Toxicol Sci* **104:**261-273.

Aleksunes LM, Slitt AL, Maher JM, Dieter MZ, Knight TR, Goedken M, Cherrington NJ, Chan JY, Klaassen CD, and Manautou JE (2006) Nuclear factor-E2-related factor 2 expression in liver is critical for induction of NAD(P)H:quinone oxidoreductase 1 during cholestasis. *Cell Stress Chaperones* **11:**356-363.

Aleksunes LM, Yeager RL, and Klaassen CD (2009) Application of multivariate statistical procedures to identify transcription factors that correlate with MRP2, 3, and 4 mRNA in adult human livers. *Xenobiotica* **39:**514-522.

Anand BS (1999) Cirrhosis of liver. *West J Med* **171:**110-115.

Baig NA, Herrine SK, and Rubin R (2001) Liver disease and diabetes mellitus. *Clin Lab Med* **21:**193-207.

Campion SN, Johnson R, Aleksunes LM, Goedken MJ, van Rooijen N, Scheffer GL, Cherrington NJ, and Manautou JE (2008) Hepatic Mrp4 induction following acetaminophen exposure is dependent on Kupffer cell function. *Am J Physiol Gastrointest Liver Physiol* **295:**G294-304.

Chen Y, Song X, Valanejad L, Vasilenko A, More V, Qiu X, Chen W, Lai Y, Slitt A, Stoner M, Yan B, and Deng R (2012) Bile salt export pump is dysregulated with altered farnesoid x receptor isoform expression in patients with hepatocellular carcinoma tissues. *Hepatology*.

Cheng Q, Aleksunes LM, Manautou JE, Cherrington NJ, Scheffer GL, Yamasaki H, and Slitt AL (2008) Drug-metabolizing enzyme and transporter expression in a mouse model of diabetes and obesity. *Mol Pharm* **5:**77-91.

Cheng X, Maher J, Dieter MZ, and Klaassen CD (2005) Regulation of mouse organic anion-transporting polypeptides (Oatps) in liver by prototypical microsomal enzyme inducers that activate distinct transcription factor pathways. *Drug Metab Dispos* **33:**1276-1282.

Doi N, Tomiyama Y, Kawase T, Nishina S, Yoshioka N, Hara Y, Yoshida K, Korenaga K, Korenaga M, Moriya T, Urakami A, Nakashima O, Kojiro M, and Hino K (2011) Focal nodular hyperplasia-like nodule with reduced expression of organic anion transporter 1B3 in alcoholic liver cirrhosis. *Intern Med* **50:**1193-1199.

Elbekai RH, Korashy HM, and El-Kadi AO (2004) The effect of liver cirrhosis on the regulation and expression of drug metabolizing enzymes. *Curr Drug Metab* **5:**157-167.

Fuchs M (2012) Non-alcoholic Fatty liver disease: the bile Acid-activated farnesoid x receptor as an emerging treatment target. *J Lipids* **2012:**934396.

Garcia-Compean D, Jaquez-Quintana JO, Gonzalez-Gonzalez JA, and Maldonado-Garza H (2009) Liver cirrhosis and diabetes: risk factors, pathophysiology, clinical implications and management. *World J Gastroenterol* **15:**280-288.

Generaux GT, Bonomo FM, Johnson M, and Mahar Doan KM (2011) Impact of SLCO1B1 (OATP1B1) and ABCG2 (BCRP) genetic polymorphisms and inhibition on LDL-C lowering and myopathy of statins. *Xenobiotica* **41:**639-651.

Hardwick RN, Fisher CD, Canet MJ, Lake AD, and Cherrington NJ (2010) Diversity in antioxidant response enzymes in progressive stages of human nonalcoholic fatty liver disease. *Drug Metab Dispos* **38:**2293-2301.

Hardwick RN, Fisher CD, Canet MJ, Scheffer GL, and Cherrington NJ (2011) Variations in ATP-binding cassette transporter regulation during the progression of human nonalcoholic fatty liver disease. *Drug Metab Dispos* **39:**2395-2402.

Hickman IJ and Macdonald GA (2007) Impact of diabetes on the severity of liver disease. *Am J Med* **120:**829-834.

Hilgendorf C, Ahlin G, Seithel A, Artursson P, Ungell AL, and Karlsson J (2007) Expression of thirty-six drug transporter genes in human intestine, liver, kidney, and organotypic cell lines. *Drug Metab Dispos* **35:**1333-1340.

Kim SJ and Kim DJ (2012) Alcoholism and diabetes mellitus. *Diabetes Metab J* **36:**108-115.

Klaassen CD and Aleksunes LM (2010) Xenobiotic, bile acid, and cholesterol transporters: function and regulation. *Pharmacol Rev* **62:**1-96.

Klaassen CD and Slitt AL (2005) Regulation of hepatic transporters by xenobiotic receptors. *Curr Drug Metab* **6:**309-328.

Lagas JS, Sparidans RW, Wagenaar E, Beijnen JH, and Schinkel AH (2010) Hepatic clearance of reactive glucuronide metabolites of diclofenac in the mouse is dependent on multiple ATP-binding cassette efflux transporters. *Mol Pharmacol* **77:**687-694.

Lieber CS, Jones DP, and Decarli LM (1965) Effects of Prolonged Ethanol Intake: Production of Fatty Liver Despite Adequate Diets. *J Clin Invest* **44:**1009-1021.

Maher JM, Aleksunes LM, Dieter MZ, Tanaka Y, Peters JM, Manautou JE, and Klaassen CD (2008) Nrf2- and PPAR alpha-mediated regulation of hepatic Mrp transporters after exposure to perfluorooctanoic acid and perfluorodecanoic acid. *Toxicol Sci* **106:**319-328.

Marek CJ, Tucker SJ, Konstantinou DK, Elrick LJ, Haefner D, Sigalas C, Murray GI, Goodwin B, and Wright MC (2005) Pregnenolone-16alpha-carbonitrile inhibits rodent liver fibrogenesis via PXR (pregnane X receptor)-dependent and PXR-independent mechanisms. *Biochem J* **387:**601-608.

More VR and Slitt AL (2011) Alteration of hepatic but not renal transporter expression in diet-induced obese mice. *Drug Metab Dispos* **39:**992-999.

More VR, Wen X, Thomas PE, Aleksunes LM, and Slitt AL (2012) Severe diabetes and leptin resistance cause differential hepatic and renal transporter expression in mice. *Comp Hepatol* **11:**1.

Moriya N, Kataoka H, Fujino H, Nishikawa J, and Kugawa F (2012) Effect of lipopolysaccharide on the xenobiotic-induced expression and activity of hepatic cytochrome P450 in mice. *Biol Pharm Bull* **35:**473-480.

Niemi M, Pasanen MK, and Neuvonen PJ (2011) Organic anion transporting polypeptide 1B1: a genetically polymorphic transporter of major importance for hepatic drug uptake. *Pharmacol Rev* **63:**157-181.

Nishimura M and Naito S (2005) Tissue-specific mRNA expression profiles of human ATP-binding cassette and solute carrier transporter superfamilies. *Drug Metab Pharmacokinet* **20:**452-477.

Nussler AK, Hao L, Knobeloch D, Yao P, Nussler NC, Wang Z, Liu L, and Ehnert S (2010) Protective role of HO-1 for alcohol-dependent liver damage. *Dig Dis* **28:**792-798.

Ogasawara K, Terada T, Katsura T, Hatano E, Ikai I, Yamaoka Y, and Inui K (2010) Hepatitis C virus-related cirrhosis is a major determinant of the expression levels of hepatic drug transporters. *Drug Metab Pharmacokinet* **25:**190-199.

Pineda Torra I, Claudel T, Duval C, Kosykh V, Fruchart JC, and Staels B (2003) Bile acids induce the expression of the human peroxisome proliferator-activated receptor alpha gene via activation of the farnesoid X receptor. *Mol Endocrinol* **17:**259-272.

Raynard B, Balian A, Fallik D, Capron F, Bedossa P, Chaput JC, and Naveau S (2002) Risk factors of fibrosis in alcohol-induced liver disease. *Hepatology* **35:**635-638.

Slitt AL, Cherrington NJ, Maher JM, and Klaassen CD (2003) Induction of multidrug resistance protein 3 in rat liver is associated with altered vectorial excretion of acetaminophen metabolites. *Drug Metab Dispos* **31:**1176-1186.

Svoboda M, Riha J, Wlcek K, Jaeger W, and Thalhammer T (2011) Organic anion transporting polypeptides (OATPs): regulation of expression and function. *Curr Drug Metab* **12:**139-153.

Syn WK, Teaberry V, Choi SS, and Diehl AM (2009) Similarities and differences in the pathogenesis of alcoholic and nonalcoholic steatohepatitis. *Semin Liver Dis* **29:**200-210.

Teng S and Piquette-Miller M (2005) The involvement of the pregnane X receptor in hepatic gene regulation during inflammation in mice. *J Pharmacol Exp Ther* **312:**841-848.

Trauner M, Arrese M, Soroka CJ, Ananthanarayanan M, Koeppel TA, Schlosser SF, Suchy FJ, Keppler D, and Boyer JL (1997) The rat canalicular conjugate export pump (Mrp2) is down-regulated in intrahepatic and obstructive cholestasis. *Gastroenterology* **113:**255-264.

Trevino LR, Shimasaki N, Yang W, Panetta JC, Cheng C, Pei D, Chan D, Sparreboom A, Giacomini KM, Pui CH, Evans WE, and Relling MV (2009) Germline genetic variation in an organic anion transporter polypeptide associated with methotrexate pharmacokinetics and clinical effects. *J Clin Oncol* **27:**5972-5978.

Tsukamoto H, Towner SJ, Ciofalo LM, and French SW (1986) Ethanol-induced liver fibrosis in rats fed high fat diet. *Hepatology* **6:**814-822.

Zollner G, Fickert P, Silbert D, Fuchsbichler A, Marschall HU, Zatloukal K, Denk H, and Trauner M (2003) Adaptive changes in hepatobiliary transporter expression in primary biliary cirrhosis. *J Hepatol* **38:**717-727.

3.7 Figure Legends

Fig. 1. Transporter mRNA expression in livers from normal, steatotic, alcohol cirrhotic, diabetic-cirrhosis, and diabetic subjects. (A) SLCO1B1, 1B3 and 2B1 mRNA expression, (B) ABCC1-6, and ABCG2 mRNA expression. Total RNA was isolated from intact human donor liver tissue (Normal, n=22; Steatosis, n=8; Alcohol cirrhosis, n=19; Diabetes, n=20; Diabetic-cirrhosis, n=9) and relative mRNA expression was quantified. Raw data was normalized to HPRT1 and log transformed before comparison. Asterisks (*) represent a statistical difference ($p \leq 0.05$) from normal non-steatotic livers and dots (●) represent outliers. SLCO1B3 mRNA expression was decreased, whereas 2B1 was increased in alcohol cirrhosis compared to normal non-steatotic livers. ABCG2, ABCC4 and 5 mRNA expression was increased in livers from donors with alcohol cirrhosis compared to normal non-steatotic livers. ABCC3 expression decreased in diabetic-cirrhosis livers.

Fig. 2. Protein expression of transporters in livers from normal, steatotic, alcohol cirrhotic, and diabetic-cirrhosis subjects by western blot. (A) Relative ABCC1-6, and ABCG2 protein expression was determined in fractions isolated from intact human liver by Western blot. Lanes 1-5 (normal, non-steatotic), 6-10 (steatosis), 11-20 (alcohol cirrhosis), and 21-25 (diabetic-cirrhosis) represent samples analyzed. (B) Quantification of western blots. Protein bands were quantified using Quantity One® software v4.6.3 (Biorad, Hercules, CA). Asterisks (*) represent a statistical difference ($p \leq 0.05$) from normal non-steatotic livers and dots (●) represent outliers. Steatosis

increased ABCC4 and ABCG2 protein expression compared to normal livers. ABCC1, 3, 5 protein expression was increased, whereas ABCC6 was decreased in alcohol cirrhotic and diabetic-cirrhotic livers as compared to normal non-steatotic livers. ABCC4 and ABCG2 expression was increased in livers with steatosis, alcohol cirrhosis and diabetic-cirrhosis.

Fig. 3. Transcription factor and biotransformation enzyme expression in livers from normal, steatotic, alcohol cirrhotic, diabetic-cirrhotic, and diabetic subjects. (A) Relative PXR, CAR, FXR and NRF2 mRNA expression in human liver. Total RNA was isolated from intact human donor liver tissue (Normal, n=22; Steatosis, n=8; Alcohol cirrhosis, n=19; Diabetes, n=20; Diabetic-cirrhosis, n=9) and relative mRNA expression was quantified. Alcohol cirrhosis and diabetic cirrhosis increased NRF2, but decreased FXR mRNA levels. Diabetic-cirrhosis also decreased PXR mRNA levels. (B) CYP3A4, 2B6, UGT1A3, and 2B7 mRNA expression in liver. Total RNA was isolated from intact human donor liver tissue (Normal, n=22; Steatosis, n=8; Alcohol cirrhosis, n=19; Diabetes, n=20; Diabetic-cirrhosis, n=9). Steatosis increased CYP3A4 and UGT1A3 mRNA expression as compared to normal non-steatotic livers. CYP2B6 mRNA expression was decreased in diabetic livers as compared to normal non-steatotic livers. (C) Relative NRF2, NQO1, and GPX1 protein expression in nuclear (NRF2) and cytosolic (NQO1, GPX1) fractions in livers of normal, steatotic, cirrhotic and diabetic-cirrhotic subjects. Lanes 1-5 (normal, non-steatotic), 6-9 (steatosis), 10-16 (alcohol cirrhosis), and 17-21 (diabetic-cirrhosis) represent samples analyzed. (D) Quantification

of NRF2, NQO1, and GPX1 western blots. Asterisks (*) represent a statistical difference ($p \leq 0.05$) from normal non-steatotic livers and dots (●) represent outliers. Nuclear NRF2 (approximately 110 kDa) and cytosolic NQO1, GPX1 protein (31 kDa and 23 kDa) levels were increased in livers of alcohol cirrhosis and diabetic-cirrhosis subjects as compared to normal livers. NQO1 was also increased in steatotic livers.

Fig. 4. Inflammatory cytokine mRNA expression in livers from normal, steatotic, alcohol cirrhotic, diabetic-cirrhotic, and diabetic subjects. Inflammatory cytokine tumor necrosis factor α (TNFα) and interleukin 1β (IL1β) mRNA expression. Steatosis increased mRNA expression of both TNFα and IL1β, and alcohol cirrhosis increased expression of only TNFα, as compared to normal non-steatotic livers.

Fig. 5. Hierarchical cluster analysis of different transporters and transcription factors. Target gene expression was normalized to HPRT1 and log transformed to use for cluster analysis. Cluster analysis was performed by using squared Pearson's correlation (R^2) as a similarity measure. Genes were clustered as a group with bigger R^2. ABCG2 and SLCO2B1 expression were closely related to CAR expression. Similarly, expression of ABCC4, ABCC5 and NRF2 were closely related to each other.

Expression of ABCC2 and PXR were also closely related, and further related to SLCO1B3 and 1B1 expression.

3.8 Tables

Table 1: Gender, ethnicity, and age information of the human liver samples used in the study

No.	Condition	Gender	Ethnicity	Age in years
1	Normal	M	Unknown	49
2	Normal	M	Unknown	45
3	Normal	F	African American	61
4	Normal	F	Caucasian	57
5	Normal	F	Caucasian	76
6	Normal	F	Caucasian	39
7	Normal	F	Caucasian	55
8	Normal	F	Caucasian	49
9	Normal	M	African American	48
10	Normal	M	Caucasian	21
11	Normal	M	Caucasian	35
12	Normal	M	Caucasian	59
13	Normal	M	Caucasian	44
14	Normal	M	Caucasian	69
15	Normal	M	Caucasian	55
16	Normal	M	Caucasian	73
17	Normal	F	Caucasian	60
18	Normal	F	Caucasian	51
19	Normal	M	Caucasian	56
20	Normal	M	Caucasian	69
21	Normal	M	Caucasian	22
22	Normal	M	Caucasian	62
23	Steatosis	M	Caucasian	37
24	Steatosis	M	Caucasian	31

25	Steatosis	M	Caucasian	46
26	Steatosis	F	Caucasian	48
27	Steatosis	F	Unknown	46
28	Steatosis	M	Caucasian	46
29	Steatosis	M	Caucasian	45
30	Steatosis	M	Caucasian	40
31	Alcohol Cirrhosis	F	Caucasian	47
32	Alcohol Cirrhosis	F	Caucasian	47
33	Alcohol Cirrhosis	F	Caucasian	44
34	Alcohol Cirrhosis	F	Caucasian	36
35	Alcohol Cirrhosis	F	Unknown	48
36	Alcohol Cirrhosis	F	Unknown	51
37	Alcohol Cirrhosis	F	Unknown	33
38	Alcohol Cirrhosis	F	Unknown	52
39	Alcohol Cirrhosis	M	Caucasian	52
40	Alcohol Cirrhosis	M	Caucasian	50
41	Alcohol Cirrhosis	M	Caucasian	44
42	Alcohol Cirrhosis	M	Caucasian	48
43	Alcohol Cirrhosis	M	Caucasian	63
44	Alcohol Cirrhosis	M	Caucasian	56
45	Alcohol Cirrhosis	M	Caucasian	55
46	Alcohol Cirrhosis	M	Unknown	42
47	Alcohol Cirrhosis	M	Unknown	33
48	Alcohol Cirrhosis	M	Unknown	46
49	Alcohol Cirrhosis	M	Caucasian	56
50	Diabetes	F	Caucasian	68
51	Diabetes	F	Asian	42

52	Diabetes	F	African American	49
53	Diabetes	F	Caucasian	51
54	Diabetes	F	Caucasian	39
55	Diabetes	F	Caucasian	72
56	Diabetes	F	Caucasian	46
57	Diabetes	F	Caucasian	74
58	Diabetes	F	Caucasian	53
59	Diabetes	F	Caucasian	38
60	Diabetes	M	Caucasian	57
61	Diabetes	M	Caucasian	48
62	Diabetes	M	African American	44
63	Diabetes	M	Caucasian	66
64	Diabetes	M	Caucasian	55
65	Diabetes	M	Caucasian	74
66	Diabetes	M	Caucasian	39
67	Diabetes	M	Caucasian	70
68	Diabetes	M	Caucasian	46
69	Diabetes	M	Caucasian	33
70	Diabetic Cirrhosis	M	Caucasian	39
71	Diabetic Cirrhosis	M	Caucasian	52
72	Diabetic Cirrhosis	M	Caucasian	36
73	Diabetic Cirrhosis	M	Caucasian	65
74	Diabetic Cirrhosis	M	Caucasian	50
75	Diabetic Cirrhosis	M	Caucasian	57
76	Diabetic Cirrhosis	M	Unknown	56
77	Diabetic Cirrhosis	M	Unknown	62
78	Diabetic Cirrhosis	M	Caucasian	52

Table 2: Type, dilution, molecular weight and source of primary antibodies for western blot analysis

Antibody	Type	Dilution	Mol wt	Source
ABCC1	MRPr1	1:2000	~190	Dr. G. Scheffer, VU Medical Center, Amsterdam
ABCC2	M_2III-5	1:600	~190	Chemicon International- Millipore, MA
ABCC3	M_3II-2	1:2000	~180	Dr. G. Scheffer, VU Medical Center, Amsterdam
ABCC4	M_4I-10	1:2000	~160	Dr. G. Scheffer, VU Medical Center, Amsterdam
ABCC5	M_5I-60	1:1000	~160	Dr. G. Scheffer, VU Medical Center, Amsterdam
ABCC6	M_6II-68	1:1000	~165	Dr. G. Scheffer, VU Medical Center, Amsterdam
ABCG2	BXP-53	1:2000	~75	Dr. G. Scheffer, VU Medical Center, Amsterdam
NQO1	Ab2346	1:5000	~30	Abcam, Cambridge, MA
GPX1	AB16798	1:2000	~27	Abcam, Cambridge, MA
NRF2	SC13032	1:1000	~110	Santa Cruz Biotech. Inc, Santa Cruz, CA
GAPDH	D16H11	1:2000	~37	Cell Signaling Technology, Danvers, MA

3.9 Figures

Figure 1: Transporter mRNA expression in livers from normal, steatotic, alcohol cirrhotic, diabetic-cirrhosis, and diabetic subjects

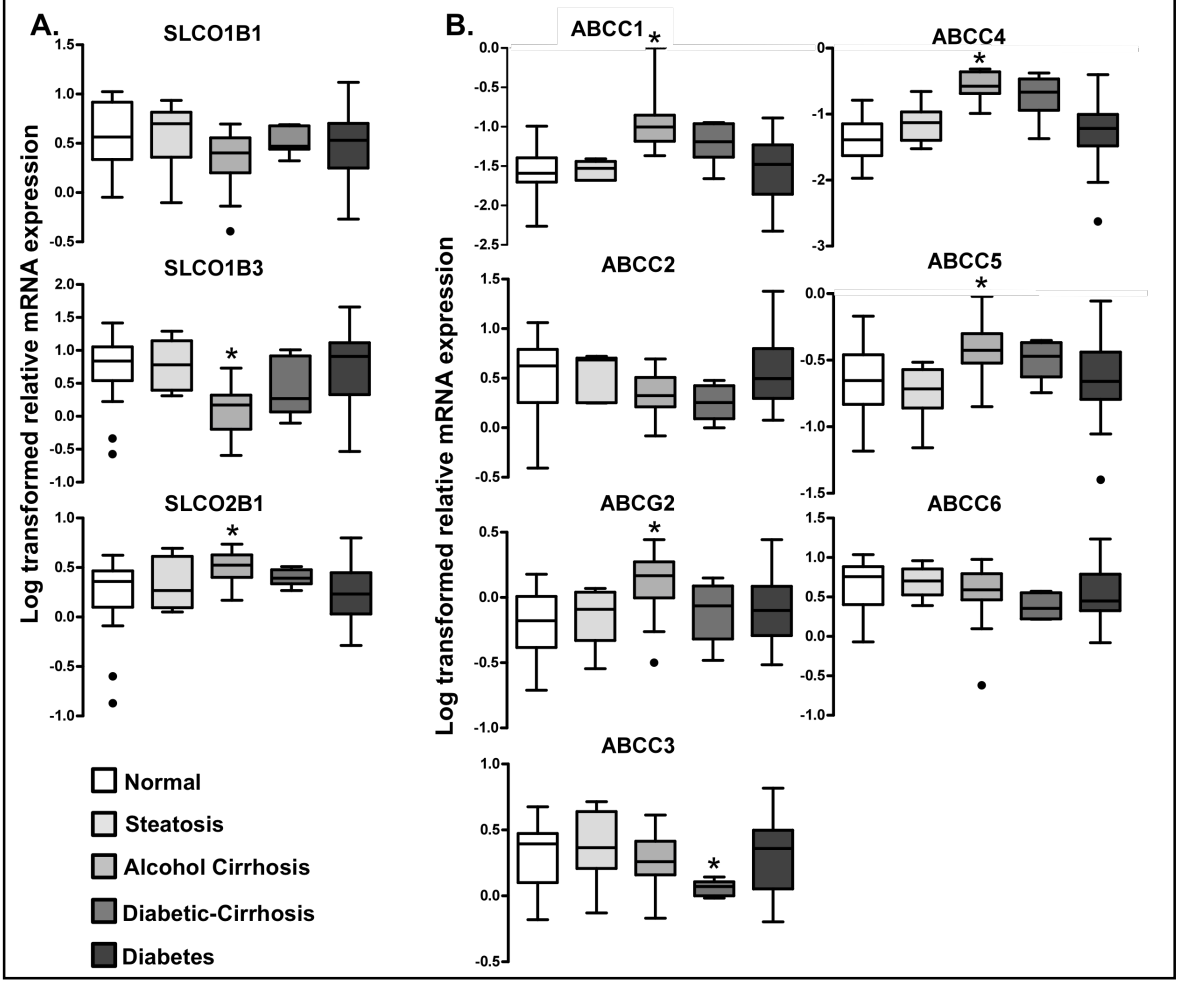

Figure 2: Protein expression of transporters in livers from normal, steatotic, alcohol cirrhotic, and diabetic-cirrhosis subjects by western blot

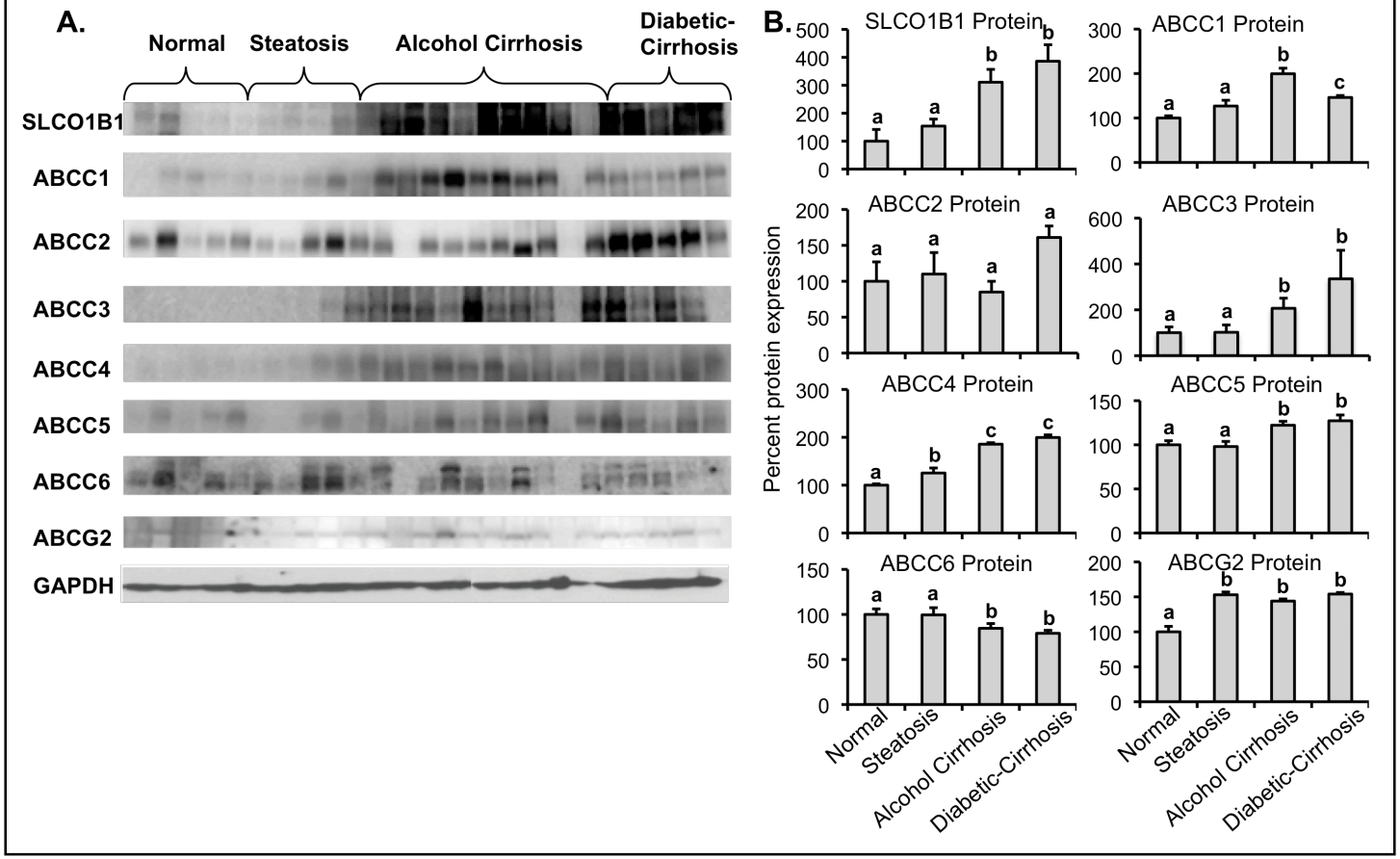

Figure 3: Transcription factor and biotransformation enzyme expression in livers from normal, steatotic, alcohol cirrhotic, diabetic-cirrhotic, and diabetic subjects

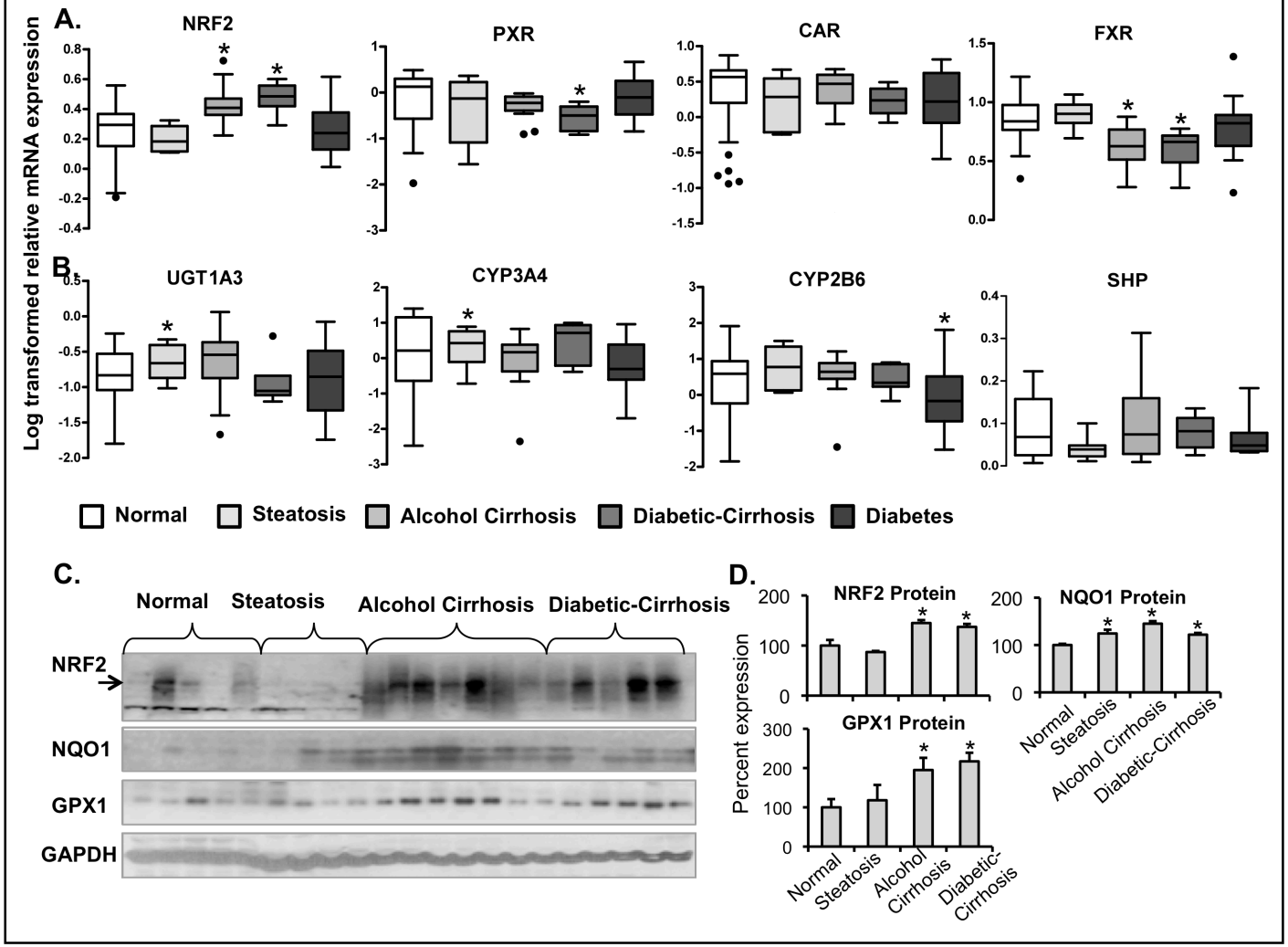

Figure 4: Inflammatory cytokine mRNA expression in livers from normal, steatotic, alcohol cirrhotic, diabetic-cirrhotic, and diabetic subjects

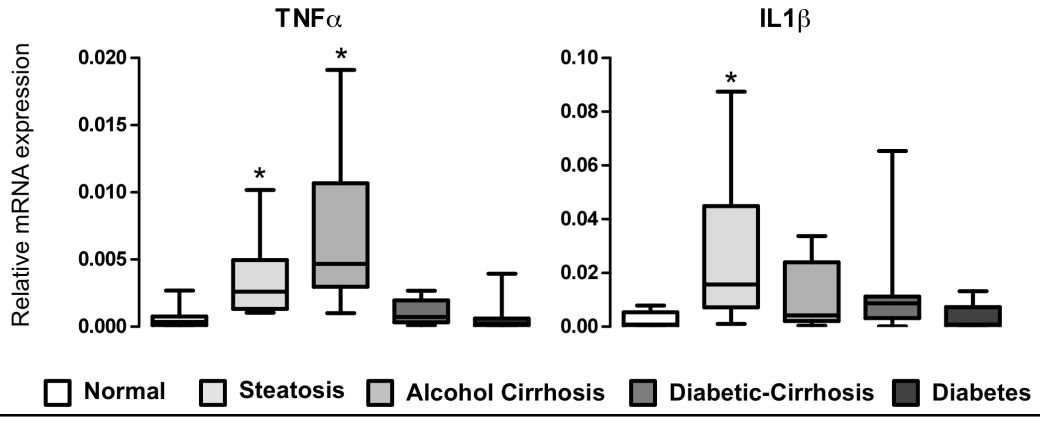

Figure 5: Hierarchical cluster analysis of different transporters and transcription factors

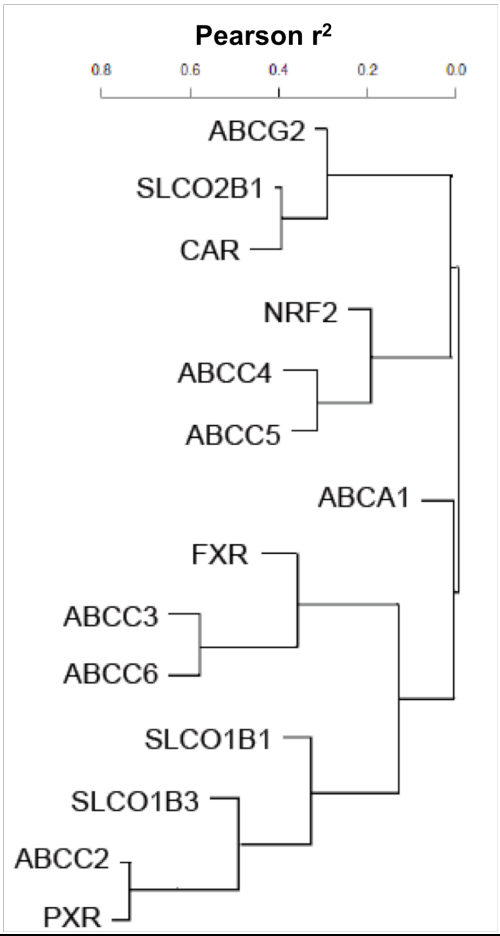

MANUSCRIPT 4

ALTERED DISPOSITION OF BISPHENOL-A IN DIET-INDUCED OBESE MICE

Vijay R More[1], Jialin Xu[1], Olivia DiPrete[1], Daniel Doerge[2], Ayman El-Kattan[1,3], Angela L Slitt[1]

[1]Biomedical and Pharmaceutical Sciences, University of Rhode Island, Kingston, RI; [2]National Center for Toxicological Research, US Food and Drug Administration, Jefferson, AZ; [3]Department of Pharmacokinetics, Dynamics and Metabolism, Pfizer Global Research and Development, Groton, CT

Formatted for submission to *J Biochemical and Molecular Toxicology (JBMT)*

4.1 Abstract:

Obesity is a global pandemic, spanning over 35% of the US population. Various mouse models of obesity have been proposed and are used in the pharmacokinetic studies. Diet-induced obese (DIO) mice are diet containing 60% kCal fat since the weaning. These mice are overweight, moderately hyperglycemic and mildly hyperinsulinemic. It was demonstrated that these mice have altered hepatic transporter expression. The purpose of this study was to study disposition of environmental chemical Bisphenol-A (BPA) in DIO mice and compare it with lean controls. The DIO mice were administered 100mg/kg body weight dose of BA-d6 orally, and the blood was collected at 0.25, 0.5, 1, 2, 4 and 8-hour time points. The serum was analyzed for BPA and its major metabolite monoglucuronide. DIO mice cleared BPA-glucuronide from the blood at much faster rate as compared to lean mice. Although BPA aglycone levels were high in DIO mice serum, total BPA levels remained lower that lean mice owing to extensive metabolism. However, enterohepatic recirculation was increased in DIO mice, causing higher total BPA in serum at later time points. These alterations in BPA disposition can be attributed to increase in hepatic apical efflux transporter Abcc2 expression, along with increased conjugation enzymes Ugt expression in DIO mice.

4.2 Introduction:

Bisphenol A (BPA) is an industrial chemical used in the polycarbonate plastic and epoxy resins manufacture. Plastic water bottles, food and beverage cans and dental sealant liners made with epoxy resins release the monomer BPA in the contents of the container in smaller amounts that leads to human exposure (1). Polyvinyl chloride plastics and thermal paper recycling also uses BPA. Although consumption through diet and water is the primary source of human exposure, BPA can also get into body through skin contact with dust, water and air (2). Owing to use of baby bottles, and other plastic products, infants and children have higher exposure as compared to adult population (2).

There are multitudes of evidences in the literature reporting harmful effects after exposure to BPA. Richter et al., reviewed toxicity of BPA after exposure to adults, as well as developmental effects when exposed from gestation through puberty (3). Harmful effects of BPA, depending on varying doses and different times of exposure, range from neuroendocrine disturbances, behavioral effects, reproductive abnormalities, gonadal development and fertility alterations in both genders and developmental effects on metabolism and immunity (3).

As toxic effects of BPA depend largely on dose and route of administration, its pharmacokinetics is under investigation in various rodent models as well as humans. According to Center for Disease Control and prevention (CDC),

more than 90% of the US population is chronically exposed to BPA (4). Therefore, in order to assess the susceptibility of all population groups, knowing the metabolism and disposition pathways of BPA becomes important (4).

Absorption of BPA to blood is very rapid and thorough, as peak concentrations of total BPA were obtained within 20 minutes of administering orally in rats. It is absorbed from small intestine, and there is conjugation of BPA to BPA glucuronide in the enterocytes (5). Plasma protein binding of BPA is extensive with the unbound fraction measuring as low as 0.046 in rats after oral administration (6). Monoglucuronide is the major metabolite of BPA. When studied in human liver microsomes, and in recombinant human UGT isoforms, it was demonstrated that UGT2B7 and 2B15 were the isoform primarily involved in BPA glucuronidation (7). In rats, BPA is predominantly conjugated by Ugt2b1 isoform (8). Membrane transporters involved in disposition of BPA-glucuronide are multidrug resistance associated protein 3 (ABCC3) in humans and Abcc2 in rats (9). As reviewed by Willhite et al (2008), as much as 80% of administered BPA is excreted in bile in rodents, as opposed to urine in humans, and there is marked enterohepatic recirculation (10).

Obesity and the complications associated with it are widespread pandemics of the modern time. Dietary and lifestyle changes are causing the positive energy balance leading to overweight and obesity (11). According to National Health and Nutrition Examination Survey (NHANES) for 2009-2010, about 36% of the adult and 17% of the young US population was obese. Diet-

induced obese (DIO) mouse is one of the commonly used rodent models of obesity. The mice are fed diet containing high fat content (60% kCal) starting from 6 weeks of age. By 13 weeks of age, the mice have about 15% more body fat content as compared to respective lean controls fed 10% kCal fat (12). These mice present with mild to moderate hyperglycemia and hyperinsulinemia.

We previously demonstrated that DIO mice are characterized by alterations in the hepatic drug transporter expression (13). As reviewed by Klaassen and Aleksunes, drug transporters are the membrane proteins, which aid in exchange of drugs, endogenous chemicals and/or metabolites exchange across the cell membrane (14). Alterations in transporter expression are known to cause differences in disposition of certain xenobiotics including acetaminophen, ezetimibe, morphine, and raloxifene (15-18). In the present study, we have characterized differential metabolism and disposition of BPA in DIO mice. In order to address the reasons for the altered BPA disposition, we have also characterized hepatic conjugation enzyme and intestinal transporter expression in DIO mice.

4.3 Materials and methods:

4.3.1 Animals: Twenty one week old C57BL/6 male mice fed 10% (Lean) or 60% kCal (DIO) fat diet (Research Diets Inc, New Brunswick, NJ) since weaning, were purchased from Jackson Laboratories (Bar Harbor, ME). The animals were allowed to acclimate for 2 week, while maintaining the same diets. For the BPA disposition study, the study design is described in table 1. Another group of mice (n=6 lean and 6 DIO) were euthanized at 23 weeks of age and liver and intestine tissues were collected.

4.3.2 BPA disposition study: As described in table 1, study used n=6 mice per group per time point. The mice were housed in individual cages, with ad libitum food and water. Deuterated BPA (BPA-d6) solution was prepared as previously described (19). Briefly, the weighed amount of BPA-d6 was dissolved in 95% ethanol before dilution in water. The solution was administered by oral gavage to mice to get 100μg/kg body weight. For each time point, the blood was collected from mice and spun to get serum.

4.3.3 BPA-d6 analysis by LC-ES/MS/MS: The detailed method for the detection of BPAd-6 is described elsewhere (20). Briefly, labeled internal standard ($^{13}C_{12}$) was added to each thawed serum sample. The samples were the purified by supported liquid extraction and analyzed by LC-ES/MS/MS in the multiple reaction-monitoring mode by monitoring specific transitions for d-6 and $^{13}C_{12}$ -BPA. Conjugated BPA was hydrolyzed by using *H. pomacia* glucuronidase/ sulfatase (Sigma Chemical Co., St. Louis, MO) incubation, and

then total amount of BPA-d6 was quantified. Subtraction of total and conjugated BPA-d6 values provided conjugated amounts. Limit of detection for BPA-d6 with this method was approximately 0.2nM (19).

4.3.4 Total RNA extraction and mRNA quantification: Total RNA was extracted from liver and intestinal tissues by phenol-chloroform extraction as described previously (21). One microgram of total RNA was converted to single-stranded cDNA by using oligo$(dT)_{18}$ primers. Quantitative real-time PCR with Roche LightCycler 480 was used to quantify mRNA expression levels. Samples were run using SYBR green and 18S was used as a housekeeping gene to normalize the raw data. The primers used are listed in the table 2. All the oligonucleotides were synthesized by Life Technologies (Grand Island, NY).

4.4 Results and discussion:

As demonstrated in fig. 1, oral administration of BPA-d6 caused rapid absorption. Cmax was achieved at earliest time point (t=0.25hrs) for both aglycone and glucuronide. Aglycone declined rapidly after achieving Cmax, indicating rapid distribution/ conjugation. AUC values for aglycone were much lower as compared to total and glucoronide form, indicating extensive metabolism. When disposition in lean and DIO mice was compared, it was observed that total BPA amounts in serum were lower in DIO mice over a period of 8 hrs after oral dosing. Lower amounts of total BPA in serum of DIO mice can be attributed to lower amounts of BPA-conjugate, as BPA is extensively metabolized. BPA conjugate measured in this study includes both BPA-glucuronide and BPA-sulfate metabolites, however as reviewed elsewhere, BPA-glucuronide is the dominant metabolite (10).

Lower levels of total BPA in DIO mice could result from the combination of multiple factors. This experiment was conducted with parallel dosing of 6 lean and 6 DIO mice per time point. So the blood levels are not from serial draws from same animal, rather these are different animals at each time point. The mice had access to food throughout the duration of the study. As mentioned earlier, DIO mice are fed a 60% kCal fat diet, whereas lean mice get diet containing only 10% kCal fat. BPA is a moderately hydrophobic with its n-octanol/ water partition coefficient more than 3. Presence of high fat diet in the gut lumen may play a role in lowered absorption of orally administered BPA. After absorption, the BPA may undergo glucoronidation within the enterocytes.

It was reported that rat intestinal microsomal preparations possessed higher conjugation activity for BPA as compared to human intestinal microsomes (22). However, little is known about extent to which mouse enterocytes glucuronidate BPA.

Because of hydrophobic nature of BPA, its transport through the membrane is thought to occur by passive diffusion (23). However, there are reports of BPA aglycone being a substrate for rat Abcc2, human ABCC2, ABCG2 and ABCC3 (24). BPA-glucuronide is a substrate for rat Abcc2, human ABCC3, but is a non-substrate/ inhibitor for human ABCC2, ABCB1, ABCG2, rat Abcb1a, Abcb1b, and Abcg2 (24). As reviewed by Willhite et al., BPA-glucuronide is preferentially excreted in bile in rats, whereas in urine in humans. This can be attributed to localization of rat Abcc2 on the apical membrane and human ABCC3 on the basolateral membrane in hepatocytes (14).

Figure 2A demonstrates alterations in efflux transporter expression in duodenum of lean and DIO mice. It was demonstrated that DIO mice have increased expression of Abcc3 and 4, and decreased expression of Abcb1, Abcc2 and Abcg2. Whether these duodenal transporters will play a role in altered disposition of BPA in DIO mice depends on extent of glucuronidation that takes place in enterocytes. In a study with segmented everted rat intestine, it was noted that increase in concentration of BPA on mucosal side increases transfer of unconjugated form to serosal side (25). Little to no information is available on intestinal BPA glucuronidation in mice.

After entering the portal circulation, BPA aglycone or glucuronide, enter the liver. In the hepatocytes, the Ugt1b isoforms specific for BPA will convert it to BPA-glucuronide, with minor sulfate conjugate formation. As demonstrated in fig. 2B, DIO mice have increased mRNA expression of Ugt1a1, 3a1 and 3a2, and increasing trend in Ugt2a3 and 2b1 as compared to lean mice. This suggests higher glucuronide formation in DIO mice as compared to lean. However, the glucuronide levels in the blood remained considerably lower in DIO mice as compared to lean. This can be attributed to possible substrate specificity on mouse Abcc2, and its significantly increased expression in DIO mice livers (13). Excretion of BPA-glucuronide in intestine through bile results in drop of serum glucuronide levels. At a later time point, DIO mice show slight increase in levels of BPA-glucuronide in blood, caused due to enterohepatic recirculation. When conjugated BPA reaches small intestine, it undergoes hydrolysis by intestinal b-glucuronidase enzyme, and release BPA aglycone. This aglycone is then absorbed back into the enterocytes. Now as this concentration of BPA will be much lower than original orally administered concentration, the extent of intestinal glucuronidation will me more (25). After intestinal glucuronidation, the conjugate will be preferably transported to serosal blood supply with the aid of increased basolateral efflux transporters Abcc3 and 4. This may explain why DIO mice have better enterohepatic recirculation of BPA as compared to lean mice.

4.5 Conclusion:

Overall body burden of BPA in DIO mice was significantly less as compared to lean mice. Enhanced expression of hepatic UGTs and apical efflux transporter Abcc2 can account for higher formation and excretion of BPA-glucuronide in feces, which results in lower levels of BPA-glucuronide in serum. Enhanced basolateral efflux and decreased apical efflux transporter expression in intestines of DIO mice may contribute to higher enterohepatic recirculation as compared to lean mice.

4.6 References:

1. Doerge DR, Twaddle NC, Woodling KA, Fisher JW. Pharmacokinetics of bisphenol A in neonatal and adult rhesus monkeys. Toxicol Appl Pharmacol 2010;248(1):1-11.

2. Shelby MD. NTP-CERHR monograph on the potential human reproductive and developmental effects of bisphenol A. NTP CERHR MON 2008(22):v, vii-ix, 1-64 passim.

3. Richter CA, Birnbaum LS, Farabollini F, Newbold RR, Rubin BS, Talsness CE, Vandenbergh JG, Walser-Kuntz DR, vom Saal FS. In vivo effects of bisphenol A in laboratory rodent studies. Reprod Toxicol 2007;24(2):199-224.

4. Calafat AM, Ye X, Wong LY, Reidy JA, Needham LL. Exposure of the U.S. population to bisphenol A and 4-tertiary-octylphenol: 2003-2004. Environ Health Perspect 2008;116(1):39-44.

5. Yoo SD, Shin BS, Lee BM, Lee KC, Han SY, Kim HS, Kwack SJ, Park KL. Bioavailability and mammary excretion of bisphenol a in Sprague-Dawley rats. J Toxicol Environ Health A 2001;64(5):417-26.

6. Kurebayashi H, Betsui H, Ohno Y. Disposition of a low dose of 14C-bisphenol A in male rats and its main biliary excretion as BPA glucuronide. Toxicol Sci 2003;73(1):17-25.

7. Hanioka N, Naito T, Narimatsu S. Human UDP-glucuronosyltransferase isoforms involved in bisphenol A glucuronidation. Chemosphere 2008;74(1):33-6.

8. Yokota H, Iwano H, Endo M, Kobayashi T, Inoue H, Ikushiro S, Yuasa A. Glucuronidation of the environmental oestrogen bisphenol A by an isoform of UDP-glucuronosyltransferase, UGT2B1, in the rat liver. Biochem J 1999;340 (Pt 2):405-9.

9. Nishikawa M, Iwano H, Yanagisawa R, Koike N, Inoue H, Yokota H. Placental transfer of conjugated bisphenol A and subsequent reactivation in the rat fetus. Environ Health Perspect 2010;118(9):1196-203.

10. Willhite CC, Ball GL, McLellan CJ. Derivation of a bisphenol A oral reference dose (RfD) and drinking-water equivalent concentration. J Toxicol Environ Health B Crit Rev 2008;11(2):69-146.

11. Malik VS, Willett WC, Hu FB. Global obesity: trends, risk factors and policy implications. Nat Rev Endocrinol 2012.

12. Bush EN, Shapiro R, Nuss M, Kaszubska W, Trevillyan J, Knourek-Segel V, Kennedy M, Adler A, Jirousek M, Jacobson P. Adiposity, Leptin Resistance, Hyperrphagia, Hyperglycemia, Glucose Intolerance and Insulin Resistance in C57BL/6J Mice Fed High Fat Diets. Endocrine Society Annual Meeting 2001, Poster Session 2001.

13. More VR, Slitt AL. Alteration of hepatic but not renal transporter expression in diet-induced obese mice. Drug Metab Dispos 2011;39(6):992-9.

14. Klaassen CD, Aleksunes LM. Xenobiotic, bile acid, and cholesterol transporters: function and regulation. Pharmacol Rev 2010;62(1):1-96.

15. Lickteig AJ, Fisher CD, Augustine LM, Aleksunes LM, Besselsen DG, Slitt AL, Manautou JE, Cherrington NJ. Efflux transporter expression and acetaminophen metabolite excretion are altered in rodent models of nonalcoholic fatty liver disease. Drug Metab Dispos 2007;35(10):1970-8.

16. Hardwick RN, Fisher CD, Street SM, Canet MJ, Cherrington NJ. Molecular mechanism of altered ezetimibe disposition in nonalcoholic steatohepatitis. Drug Metab Dispos 2012;40(3):450-60.

17. Trdan Lusin T, Mrhar A, Stieger B, Kullak-Ublick GA, Marc J, Ostanek B, Zavratnik A, Kristl A, Berginc K, Delic K and others. Influence of hepatic and intestinal efflux transporters and their genetic variants on the pharmacokinetics and pharmacodynamics of raloxifene in osteoporosis treatment. Transl Res 2012;160(4):298-308.

18. Hasegawa Y, Kishimoto S, Takahashi H, Inotsume N, Takeuchi Y, Fukushima S. Altered expression of ABCC2, ABCC3 and UGT2B1 in the liver affects the disposition of morphine and its glucuronide conjugate in a rat model of cholestasis. J Pharm Pharmacol 2009;61(9):1205-10.

19. Doerge DR, Twaddle NC, Vanlandingham M, Fisher JW. Pharmacokinetics of bisphenol A in serum and adipose tissue following intravenous administration to adult female CD-1 mice. Toxicol Lett 2012;211(2):114-9.

20. Twaddle NC, Churchwell MI, Vanlandingham M, Doerge DR. Quantification of deuterated bisphenol A in serum, tissues, and excreta from adult Sprague-Dawley rats using liquid chromatography with tandem mass spectrometry. Rapid Commun Mass Spectrom 2010;24(20):3011-20.

21. More VR, Wen X, Thomas PE, Aleksunes LM, Slitt AL. Severe diabetes and leptin resistance cause differential hepatic and renal transporter expression in mice. Comp Hepatol 2012;11(1):1.

22. Mazur CS, Kenneke JF, Hess-Wilson JK, Lipscomb JC. Differences between human and rat intestinal and hepatic bisphenol A glucuronidation and the influence of alamethicin on in vitro kinetic measurements. Drug Metab Dispos 2010;38(12):2232-8.

23. Balakrishnan B, Henare K, Thorstensen EB, Ponnampalam AP, Mitchell MD. Transfer of bisphenol A across the human placenta. Am J Obstet Gynecol 2010;202(4):393 e1-7.

24. Mazur CS, Marchitti SA, Dimova M, Kenneke JF, Lumen A, Fisher J. Human and rat ABC transporter efflux of bisphenol a and bisphenol a glucuronide: interspecies comparison and implications for pharmacokinetic assessment. Toxicol Sci 2012;128(2):317-25.

25. Inoue H, Yuki G, Yokota H, Kato S. Bisphenol A glucuronidation and absorption in rat intestine. Drug Metab Dispos 2003;31(1):140-4.

4.7 Figure legends:

Figure 1. Serum BPA-d6, conjugates, and total time-concentration profile in lean and DIO mice after oral administration of 100mg/kg body weight BPA-d6. Dosing of animals from all six time-points was completed within 45 minutes. The serum was extracted and BPA-d6 (before and after incubation with glucuronidase/sulfatase mix) was quantified by LC-ES/MS/MS using $^{13}C_{12}$ as an internal standard. * indicates statistical significance in AUC between lean and DIO mice ($p<0.05$).

Figure 2. Messenger RNA expression of UDP glucuronosyl transferases (Ugts) in liver and efflux transporters in duodenum of lean and DIO mice. Total RNA was isolated from liver/ duodenal tissue by phenol-chloroform extraction, and mRNA was quantified by Quantitative Real-Time PCR, using SYBR green. **A)** Canalicular efflux transporters Abcc2, Abcb1, Abcg2 and basolateral efflux transporters Abcc3 and 4 mRNA expression in duodenum. **B)** Ugt1a1, 1a6, 2a3, 2b1, 2b5, 3a1, and 3a2 mRNA expression in liver. *indicates statistical significance in AUC between lean and DIO mice ($p<0.05$).

4.8 Tables:

Table 1: Number of animals used in Bisphenol-A (BPA) disposition study[#].

	15 min	30 min	60 min	2 hrs	4 hrs	8 hrs
Lean	6	6	6	6	6	6
DIO	6	6	6	6	6	6

[#]All the animals were age-matched (23 weeks).

Table 2: Oligonucleaotide primers used in Quantitative Real-Time PCR[$]

mUgt1a1 forward	GCTTCTTCCGTACCTTCTGTTG
mUgt1a1 reverse	GCTGCTGAATAACTCCAAGCAT
mUgt1a6 forward	GTTTCTCTTCCTAGTGCTTTGGG
mUgt1a6 reverse	CCTCGTTCACTGAGATGTTCTAC
mUgt2b1 forward	GTGCTGGTGTGGCCTACAG
mUgt2b1 reverse	ATTGCTCGGCCCAATGAGG
mUgt2a3 forward	CGTGTGGCCCTGTGATATGAG
mUgt2a3 reverse	GTGCAGTGGAATACGTTTACTCT
mUgt2b5 forward	ACGAGGCGATCTATCATGGAA
mUgt2b5 reverse	GACCTCCTCCAGTGCATTGAG
mUgt3a1 forward	AAACGCCCCCTTGTCATATG
mUgt3a1 reverse	CCTTCGCTTCTTGGTGAAATG
mUgt3a2 forward	CACTCATGGAGGGATGAACAGT
mUgt3a2 reverse	TGGTGAGCGCAAATGACTCTG

[$]Synthesized by Life Technologies (Grand Island, NY)

4.9 Figures:

Figure 1: Serum BPA-d6, conjugates, and total time-concentration profile in lean and DIO mice after oral administration of 100mg/kg body weight BPA-d6

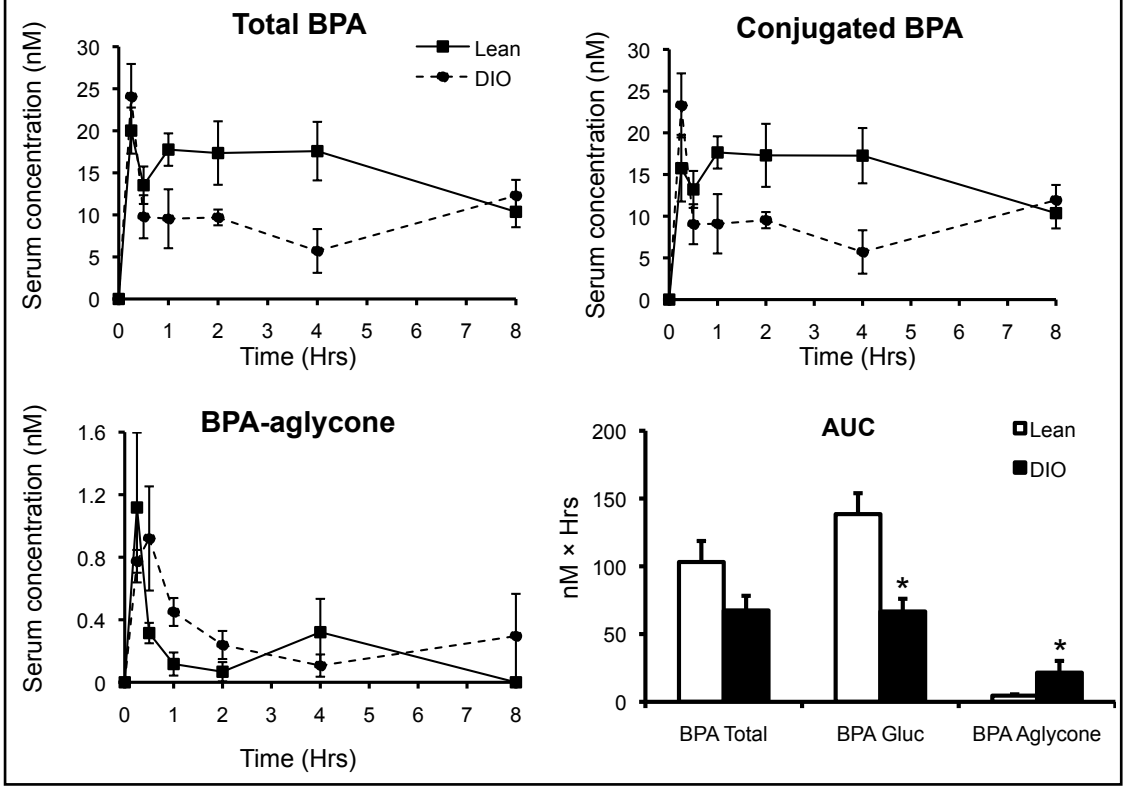

Figure 2: . Messenger RNA expression of UDP glucuronosyl transferases (Ugts) in liver and efflux transporters in duodenum of lean and DIO mice

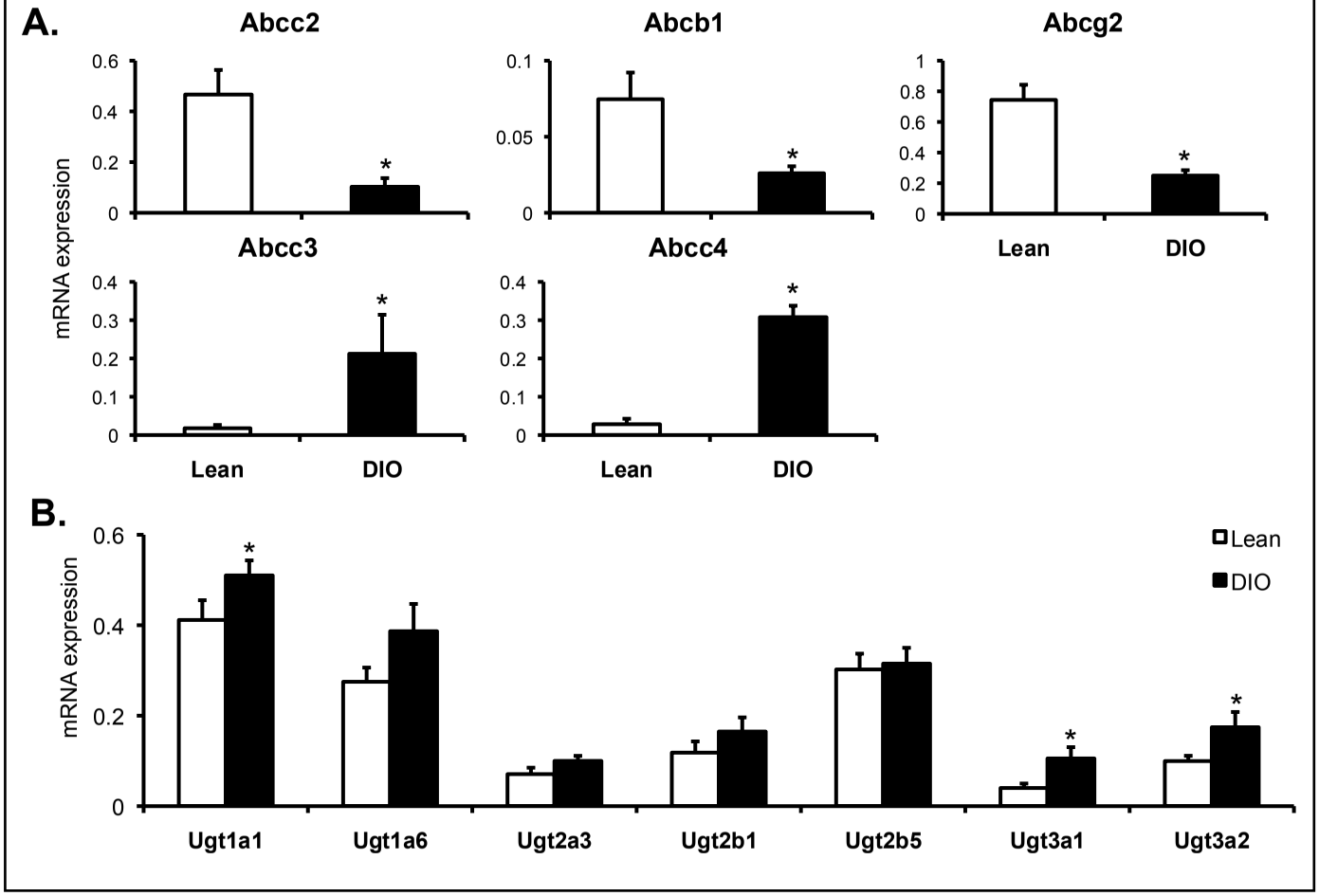

SUMMARY AND CONCLUSION

1. Constitutive activation of Nrf2 makes mice susceptible to development of diet-induced obesity, steatosis and glucose intolerance.

2. Along with role in combating oxidative stress, it appears that Nrf2 also regulates some key events in steatosis of the liver, and more studies are needed to clarify the mechanism behind these observations.

3. Alcohol cirrhosis increases the expression of efflux transporters in human liver. Alterations in expression of these transporters may alter the disposition of xenobiotics that are substrates for the transporters. Expression of nuclear factors NRF2, FXR and PXR was also altered and a correlation was observed between nuclear factors and transporter expression with disease conditions. Altered disposition abilities of patients with alcohol cirrhosis should be taken into consideration when addressing adverse drug events and drug-drug interactions.

4. Diet-induced obesity alters phase II conjugation enzymes and intestinal drug transporter expression in mice. DIO mice have enhanced clearance and high enterohepatic recirculation environmental chemical Bisphenol A. This can be attributed to alterations in hepatic phase II conjugation enzymes, hepatic transporters and intestinal transporter expression alterations in this model.

5. In summary, two distinct roles of Nrf2 were demonstrated- a role in development of steatosis with HFD treatment; and regulation of transporter expression in response to disease conditions like alcohol cirrhosis.